Pergamon

Int. J. Solids Structures Vol. 31, No. 12/13, pp. 1793–1827, 1994
Elsevier Science Ltd
Printed in Great Britain
0020–7683/94 $7.00 + .00

0020–7683(93)E0011–6

DESIGN SENSITIVITIES IN PROBLEMS INVOLVING MATERIAL AND GEOMETRIC NONLINEARITIES

S. MUKHERJEE and Q. ZHANG
Department of Theoretical and Applied Mechanics, Kimball Hall, Cornell University, Ithaca, NY 14853, U.S.A.

Abstract—The subject of this paper is the determination of design sensitivity coefficients (DSCs) for linear (elasticity) and nonlinear (both material and geometric) problems in solid mechanics. DSCs here refer to rates of change of response variables such as displacements or stresses in a deforming solid body, with respect to parameters (called design variables) that control the initial, undeformed shape of the body. In nonlinear problems, these DSCs are history dependent.

The direct differentiation approach (DDA) of the relevant derivative boundary element method (DBEM) formulation is employed here to obtain the DSCs. Modelling of sharp corners on the boundary of a body is given special attention here. Numerical results are presented for illustrative examples. The numerically obtained sensitivities, even for stresses on the boundary of a body, are shown, in general, to be very accurate. Typically, it is difficult to obtain DSCs for boundary stresses accurately by other methods—yet they are very useful for optimal shape design of bodies.

Ongoing research is currently focused on numerical calculation of DSCs for large deformation problems and use of these DSCs in process optimization. An important future application area of this work is optimal design of manufacturing processes such as extrusion or forging.

1. INTRODUCTION

This paper presents some recent formulations and numerical results for the calculation of design sensitivity coefficients (DSCs), for solid mechanics problems, by boundary element methods. The primary focus is DSCs for nonlinear problems—both material (elasto-plasticity and elastoviscoplasticity) and geometric (large strain–large rotation). For completeness, some results for linear elasticity are included as well.

DSCs are rates of change of response quantities such as stress or displacement, with respect to design variables. These design variables could be shape parameters that control the (initial) shape of part or whole of the boundary of a body, or they could be boundary conditions, material parameters, etc. Shape parameters as design variables are of concern in this work.

DSCs are useful in diverse problems. An example is a design problem where the performance of a modified design can be obtained from that of an initial design using a Taylor series expansion about the initial design. They are useful in solving inverse problems (Zabaras *et al.*, 1988) and reliability analyses (Ang and Tang, 1975). A very important application area of DSCs with respect to shape parameters is in optimal shape design. An optimization process starts with a preliminary design and calculation of DSCs for this design. This information is the input to an optimization computer program. Such a non-linear programming algorithm (for example Vanderplaats, 1983) uses the preliminary design and its sensitivities to propose a new design. The goal is to optimize an objective function without violating the constraints (typically allowable stresses or displacements) of a problem. This process is carried out in an iterative manner, producing a succession of designs, until an optimal design is obtained.

There is a rich literature on the subject of determination of DSCs for linear problems in mechanics such as elasticity or heat transfer (see, for example, Haug *et al.*, 1986).

Basically, three different approaches have been used—the finite difference approach (FDA), the adjoint structure approach (ASA) and the direct differentiation approach (DDA). Also, both the finite element method (FEM) and the boundary element method (BEM) have been used for these analyses by different researchers.

Attention is now focussed on a very promising approach—the DDA of the governing boundary integral equations of a problem. Here, the exact differentiation eliminates errors that might occur from the use of finite differencing and leads to closed form integral equations for desired sensitivities. These equations are then solved by numerical discretization. This approach is very accurate and efficient.

Recently, a number of researchers have published papers on the determination of DSCs for linear elastic problems by the BEM. These include planar (Barone and Yang, 1988; Kane and Saigal, 1988; Zhang and Mukherjee, 1991a), axisymmetric (Saigal *et al.*, 1989; Rice and Mukherjee, 1990) and three-dimensional (Barone and Yang, 1989; Aithal *et al.*, 1991) problems. Work on second order DSCs for linear elasticity problems has been recently completed by Zhang and Mukherjee (1991b).

While most of the BEM work cited above uses the standard BEM equations (see, for example, Mukherjee, 1982), the work of Zhang and Mukherjee is based on a derivative boundary element (DBEM) approach. This formulation, presented by Ghosh *et al.* (1986) and Ghosh and Mukherjee (1987), uses tractions and displacement derivatives (rather than tractions and displacements) as primary variables on the boundary of a body. This idea has two significant advantages over the standard BEM. The first is that the kernels are only logarithmically singular for two-dimensional elasticity problems. These weakly singular kernels can be integrated very accurately by log-weighted Gaussian integration. Extremely accurate integration of singular functions is an essential requirement for accurate determination of sensitivities, as will be elaborated upon later in this chapter. The second advantage is that boundary stresses can be obtained from the boundary values of tractions and displacement derivatives by purely algebraic calculations. This allows one to determine stresses and their sensitivities, on the boundary of a body, with great accuracy. Also, use of this idea allows an exact treatment of corners and zones in a body (Zhang and Mukherjee, 1991a,b).

The problem of DSCs for nonlinear solid mechanics problems has only recently begun to attract attention. Arora and his co-workers (Wu and Arora, 1987; Cardoso and Arora, 1988; Tsay and Arora, 1990; Tsay *et al.*, 1990) and Tortorelli (1988, 1990) have attempted nonlinear sensitivity problems with the FEM. Mukherjee and Chandra (1989, 1991), in two recent papers, have presented mathematical formulations, based on the BEM, for the same class of problems. The first paper (Mukherjee and Chandra, 1989) deals with small strain elastoplastic or elastoviscoplastic problems, while large strains and rotations are included in the formulation presented in the second paper (Mukherjee and Chandra, 1991). Numerical results for DSCs for small strain elastoviscoplastic problems have just been obtained by Zhang *et al.* (1991). Inclusion of material and geometrically nonlinear effects opens new doors in DSCs and optimization research, in that optimization of processes, rather than just products, can now be attempted. One can, for example, attempt to optimize the shape of a die for extrusion or the shape of a pre-form for forging. The problems, however, become quite complicated, since nonlinearities come into the picture and the response variables, and therefore their sensitivities, now become history dependent. Also, since nonelastic strain rates are typically strongly nonlinear and sensitive functions of stresses, and DSCs are derivatives of the history dependent response variables, the numerical process must be extremely accurate in order to deliver meaningful results for the desired DSCs. In fact, in order to obtain the elastoviscoplastic results presented later in this chapter (from Zhang *et al.*, 1991), even a half per cent numerical error in some integrals of logarithmically singular functions proved to be intolerable and the integration algorithm had to be improved even further. The BEM, on the other hand, is known to be extremely accurate, if it is implemented with care. Thus, the DDA of the BEM has very strong potential for success in solving these complicated problems with sufficient accuracy.

This chapter begins (Section 2) with a short discussion of the standard BEM equations and the corresponding sensitivity formulation based on the work of Barone and Yang

(1988, 1989) and Rice and Mukherjee (1990). This is followed by a presentation of a derivative boundary element (DBEM) approach for the determination of DSCs for linear elasticity problems. The issue of modelling of corners on the boundary of a body is addressed here. Numerical examples are presented for the sensitivity of stress at the vertex of a wedge, with respect to the wedge angle, as well as sensitivities of stresses in a plate with an elliptical hole, with respect to the semimajor axis of the ellipse.

The subject of Section 3 is sensitivities for elastoplastic and elastoviscoplastic problems with small strains and rotations (material nonlinearities only). The governing DBEM equations of the problem are presented first and these are followed by the sensitivity equations. The corner equations, in the presence of plasticity, are presented next. Finally, numerical results are presented for one-dimensional problems as well as for the expansion of a hollow disc. A viscoplastic constitutive model due to Anand (1982) is employed to describe material behavior in these numerical examples.

Section 4 addresses fully nonlinear problems. Here, elastic strains are assumed to be small (as is usually the case for the deformation of metallic bodies) but nonelastic strains and rotations can be arbitrarily large. An updated Lagrangian formulation is used for the mechanics problem. The sensitivities, however, are described with respect to changes in the initial geometry. Thus, it is best to view this aspect of the problem from a total Lagrangian framework. The goal here is to determine the histories of sensitivities of stresses and displacements in a solid undergoing large deformations, such as in metal forming, with respect to perturbations in the initial shape of the body.

The chapter concludes with some concluding remarks.

2. LINEAR ELASTICITY

2.1. *The standard BEM formulation and sensitivity equations*

The well known boundary integral equation for isotropic linear elastic solids, in two or three dimensions, has the form (Rizzo, 1967)

$$\mathbf{C}_{ij}(P)u_i(P) = \int_{\partial B} [U_{ij}(P, Q)\tau_i(Q) - T_{ij}(P, Q)u_i(Q)]\, \mathrm{d}s(Q), \tag{1}$$

where u_i and τ_i are the components of the displacement and traction vectors, respectively, on the boundary ∂B of a body and U_{ij} and T_{ij} are the Kelvin kernels for a point force in an infinite body. These kernels, for two or three dimensions, are available in many references (e.g. Mukherjee, 1982). Also, P is a source point and Q is a field point on the boundary ∂B and $\mathrm{d}s$ is a surface (or line) element on it.

The corner tensor $\mathbf{C}_{ij}$ arises from the kernel T_{ij}. Its value is $1/2\delta_{ij}$ (where δ_{ij} is the Kronecker delta) at a point P where ∂B is locally smooth. Otherwise, it can be proved to be

$$\mathbf{C}_{ij}(P) = -\int_{\partial B} T_{ij}(P, Q)\, \mathrm{d}s(Q). \tag{2}$$

Explicit expressions for $\mathbf{C}_{ij}$ for plane strain or for plane stress are available elsewhere (e.g. Mukherjee, 1982).

At this point it is convenient to replace $\mathbf{C}_{ij}$ in eqn (1) by using eqn (2). The result is:

$$0 = \int_{\partial B} [U_{ij}(P, Q)\tau_i(Q) - T_{ij}(P, Q)(u_i(Q) - u_i(P))]\, \mathrm{d}s(Q). \tag{3}$$

Barone and Yang (1988, 1989) have considered design sensitivities of the above problem in the absence of corners. Rice and Mukherjee (1990) have included the effect of corners in the manner shown above. It is assumed at this stage, that the shape of the body is

determined by a finite dimensional vector with components b_i and that shape changes occur continuously. Differentiating the above equation with respect to a typical b_i (here designated **b**), one obtains the sensitivity equation:

$$0 = \int_{\partial B} [U_{ij}(\mathbf{b}, P, Q)\overset{*}{\tau}_i(\mathbf{b}, Q) - T_{ij}(\mathbf{b}, P, Q)(\overset{*}{u}_i(\mathbf{b}, Q) - \overset{*}{u}_i(\mathbf{b}, P))]\, ds(\mathbf{b}, Q)$$

$$+ \int_{\partial B} [\overset{*}{U}_{ij}(\mathbf{b}, P, Q)\tau_i(\mathbf{b}, Q) - \overset{*}{T}_{ij}(\mathbf{b}, P, Q)(u_i(\mathbf{b}, Q) - u_i(\mathbf{b}, P))]\, ds(\mathbf{b}, Q)$$

$$+ \int_{\partial B} [U_{ij}(\mathbf{b}, P, Q)\tau_i(\mathbf{b}, Q) - T_{ij}(\mathbf{b}, P, Q) - u_i(\mathbf{b}, P)]\, \overset{*}{ds}(\mathbf{b}, Q), \quad (4)$$

where a superposed * denotes a derivative with respect to b. Writing:

$$T_{ij}(\mathbf{b}, P, Q) = \Sigma_{ijk}(\mathbf{b}, P, Q)n_k(\mathbf{b}, Q),$$

where n_k are the components of the unit outward normal to the boundary ∂B of B at a point Q on it, one obtains (Barone and Yang, 1988):

$$\overset{*}{U}_{ij}(\mathbf{b}, P, Q) = U_{ij,k}(\mathbf{b}, P, Q)[\overset{*}{x}_k(Q) - x_k(P)], \quad (5)$$

$$\overset{*}{T}_{ij}(\mathbf{b}, P, Q) = \Sigma_{ijk,l}(\mathbf{b}, P, Q)[\overset{*}{x}_l(Q) - \overset{*}{x}_l(P)]n_k(\mathbf{b}, Q) + \Sigma_{ijk}(\mathbf{b}, P, Q)\overset{*}{n}_k(\mathbf{b}, Q), \quad (6)$$

where $_{,k}$ denotes a field point derivative with respect to $x_k(Q)$.

A very interesting feature of the asymptotic behavior of $\overset{*}{U}_{ij}$ and $\overset{*}{T}_{ij}$ as r, the distance between P and Q, tends to zero, is that:

$$\overset{*}{U}_{ij} \sim O(1/r) \text{ for three dimensions, } \sim O(1) \text{ for two dimensions}$$

$$\overset{*}{T}_{ij} \sim O(1/r^2) \text{ for three dimensions, } \sim O(1/r) \text{ for two dimensions,}$$

by virtue of the fact that

$$\overset{*}{x}_k(Q) - \overset{*}{x}_k(P) \sim O(r).$$

Thus, the singularities in U_{ij} and T_{ij} are not enhanced by differentiation with respect to a design variable. Further, the strongest singularity in eqn (4) is $O(1/r)$ for three-dimensional problems while for two-dimensional problems it is $O(\ln r)$! Also, for two-dimensional problems,

$$\overset{*}{ds}(\mathbf{b}, Q) = [\overset{*}{x}_{k,k}(Q) - n_i n_j \overset{*}{x}_{i,j}(Q)]\, ds(\mathbf{b}, Q). \quad (7)$$

Barone and Yang have used the above approach to obtain sensitivities of planar and three-dimensional problems in their papers published in 1988 and 1989, respectively. They face some difficulty in the calculation of boundary stress sensitivities since now integrands of the type $O(1/r^2)$ for three-dimensional and $O(1/r)$ for two-dimensional must be dealt with. They employ methods of finite part integration to overcome this difficulty. The calculation of boundary stresses, and their sensitivities, is particularly simple for two-dimensional problems, if the DBEM formulation is employed. This is discussed in the next section.

2.2. *The DBEM formulation for planar problems*

2.2.1. *The DBEM equations.* Ghosh *et al.* have proposed a derivative boundary element method (DBEM) formulation for linear elasticity in which the tractions and tangential derivatives of displacements (Ghosh *et al.*, 1986, for two-dimensional problems) or tractions and displacement gradients (Ghosh and Mukherjee, 1987, for three-dimensional problems) are the primary variables on the boundary of a body. An analogous formulation has been presented also by Okada *et al.* (1988).

The BEM equations for two-dimensional linear elasticity for a simply connected region B can be written as (Ghosh *et al.*, 1986):

$$\int_{\partial B} [U_{ij}(P,Q)\tau_i(Q) - W_{ij}(P,Q)\Delta_i(Q)]\,\mathrm{d}s(Q) = 0, \tag{8}$$

where U_{ij} is the usual Kelvin kernel as before and, for plane strain:

$$W_{ij} = \frac{1}{4\pi(1-\upsilon)}[2(1-\upsilon)\psi\delta_{ij} + \gamma_{ik}r_{,k}r_{,j} + (1-2\upsilon)\gamma_{ij}\ln r]. \tag{9}$$

Here ψ is the angle between the vector $\mathbf{r}(P,Q)$ and a reference direction and Δ_i are the components of the tangential derivative of the displacement ($\partial u_i/\partial s = \Delta_i$), with s the curvilinear coordinate measured along the boundary ∂B of the planar body. Also, $\gamma_{11} = \gamma_{22} = 0$, $\gamma_{12} = -\gamma_{21} = 1$, υ is the Poisson's ratio and δ_{ij} is the Kronecker delta. It is very important to note that W_{ij} has only a logarithmic singularity (same as U_{ij}) as r goes to zero. It should be noted that for some problems with prescribed displacement on a portion ∂B_1 of ∂B, prescription of Δ on ∂B_1 might lead to loss of information on the displacement itself. This may lead to loss of uniqueness of the solution obtained from this formulation. In such cases, this difficulty can be overcome by appending a constraint equation of the type:

$$\int_A^B \Delta_i\,\mathrm{d}s = u_i(B) - u_i(A), \tag{10}$$

where A and B are suitably chosen points on the boundary ∂B.

As can be seen from eqn (8), the traction and tangential displacement derivative vectors are the primary unknowns on ∂B in this formulation. It has been shown that the stress components at a regular point on ∂B, for plane strain, can be written in terms of the components of τ and Δ as (Sladek and Sladek, 1986; Cruse and Vanburen, 1971):

$$\sigma_{ij} = A_{ijk}\tau_k + B_{ijk}\Delta_k, \tag{11}$$

where

$$A_{ijk} = (n_i n_j + c_1 t_i t_j)n_k + (n_i t_j + n_j t_i)t_k$$
$$B_{ijk} = c_2 t_i t_j t_k,$$

with $c_1 = \upsilon/(1-\upsilon)$, $c_2 = 2G/(1-\upsilon)$ and G the shear modulus of the material. Also, n_i and t_i are the components of the unit (outward) normal and (counter-clockwise) tangential vectors at a point on ∂B. Thus, if τ and Δ are primary variables on ∂B in a BEM formulation, then these quantities, as well as σ_{ij}, can be obtained on ∂B with very high accuracy.

2.2.2. *Sensitivity equations.* The corresponding DBEM equation for the sensitivities are obtained by differentiating eqn (8) with respect to a shape variable b (Zhang and Mukherjee, 1991a):

$$\int_{\partial B} [U_{ij}(\mathbf{b}, P, Q)\overset{*}{\tau}_i(\mathbf{b}, Q) - W_{ij}(\mathbf{b}, P, Q)\overset{*}{\Delta}_i(\mathbf{b}, Q)]\, ds(\mathbf{b}, Q)$$

$$+ \int_{\partial B} [\overset{*}{U}_{ij}(\mathbf{b}, P, Q)\tau_i(\mathbf{b}, Q) - \overset{*}{W}_{ij}(\mathbf{b}, P, Q)\Delta_i(\mathbf{b}, Q)]\, ds(\mathbf{b}, Q)$$

$$+ \int_{\partial B} [U_{ij}(\mathbf{b}, P, Q)\tau_i(\mathbf{b}, Q) - W_{ij}(\mathbf{b}, P, Q)\Delta_i(\mathbf{b}, Q)]\, \overset{*}{ds}(\mathbf{b}, Q) = 0, \quad (12)$$

where a superscribed * denotes a derivative with respect to a typical component of b. Now:

$$\overset{*}{W}_{ij}(\mathbf{b}, P, Q) = W_{ij,k}(\mathbf{b}, P, Q)[\overset{*}{x}_k(Q) - \overset{*}{x}_k(P)], \quad (13)$$

so that $\overset{*}{W}_{ij}$ (like $\overset{*}{U}_{ij}$) is completely regular.

A more convenient equation can be written for $\overset{*}{ds}$ (for planar problems) than eqn (7) given earlier. If the parametric equations of a curve, which is part or all of the boundary ∂B, are given by

$$x_1 = f_1(\mathbf{b}, \eta), \quad x_2 = f_2(\mathbf{b}, \eta), \quad (14)$$

where η within $[c, d]$ is a mapping parameter with c, d appropriate scalars and η independent of $\mathbf{b}$, it can be proved that (Zhang and Mukherjee, 1991a)

$$\frac{\overset{*}{ds}}{ds} = \frac{\dfrac{\partial}{\partial b}\left|\dfrac{\partial \mathbf{x}}{\partial \eta}\right|}{\left|\dfrac{\partial \mathbf{x}}{\partial \eta}\right|}, \quad (15)$$

where $|\ |$ denotes the length of the vector under consideration.

A very interesting feature of eqn (12) is that its first line is identical to eqn (8) with the sensitivities replacing the tractions and displacement derivatives. Analogous to the usual BEM problem, half of the sensitivities on ∂B must be prescribed and the rest can then be determined from eqn (12). Thus, the sensitivity problem has the same coefficient matrices as the original BEM problem with a known right hand side (since τ and Δ on ∂B are known at this stage). This known right hand side involves the evaluation of regular integrals which is very easy to perform accurately.

The equation for the sensitivity of stress at a regular point on ∂B is obtained by differentiating eqn (11) with respect to the design variable $\mathbf{b}$

$$\overset{*}{\sigma}_{ij} = A_{ijk}\overset{*}{\tau}_k + B_{ijk}\overset{*}{\Delta}_k + \overset{*}{A}_{ijk}\tau_k + \overset{*}{B}_{ijk}\Delta_k. \quad (16)$$

The above equation expresses $\overset{*}{\sigma}_{ij}$ as a linear combination of $\overset{*}{\tau}_i$, $\overset{*}{\Delta}_i$ and their sensitivities. Hence, one expects $\overset{*}{\sigma}_{ij}$ to be obtained as accurately as $\overset{*}{\tau}_i$ and $\overset{*}{\Delta}_i$.

It should be noted that $\overset{*}{A}_{ijk}$ and $\overset{*}{B}_{ijk}$ involve sensitivities of geometrical quantities such as the normal $\mathbf{n}$ to ∂B. Convenient formulae for n_i and $\overset{*}{n}_i$ can be written as [see eqn (14)] $(i = 1, 2)$

$$n_i = \frac{\gamma_{ij}\dfrac{\partial x_j}{\partial \eta}}{\left|\dfrac{\partial \mathbf{x}}{\partial \eta}\right|}, \quad \overset{*}{n}_i = \frac{\gamma_{ij}}{\left|\dfrac{\partial \mathbf{x}}{\partial \eta}\right|}\left[\frac{\partial}{\partial b}\left(\frac{\partial x_j}{\partial \eta}\right) - \frac{\partial x_j}{\partial \eta}\frac{\overset{*}{\mathrm{d}s}}{\mathrm{d}s}\right], \tag{17}$$

where $\overset{*}{\mathrm{d}s}/\mathrm{d}s$ is given in eqn (15) and γ_{ij} appears in eqn (9). Since $t_1 = -n_2$ and $t_2 = n_1$, the formulae for t_i and $\overset{*}{t}_i$ have exactly the same forms as eqn (17) with the Kronecker delta, δ_{ij}, replacing γ_{ij}.

2.2.3. *Modelling of corners.* A real solid body may include some corners across each of which there is a jump in the unit vectors **n** and **t** which are normal and tangential to the boundary ∂B (Fig. 1). Consequently, discontinuities in both the tractions and tangential derivatives of displacements will occur at a corner. Therefore, eight quantities are of interest at a corner in the two-dimensional elasticity problem, only four of which are prescribed from the boundary conditions. If a source point P is placed exactly at a corner (conforming boundary elements) one obtains two BEM equations at P, but two more independent equations are still necessary. Fortunately, this information can be obtained by considering the behavior of stress components at a corner point.

The stress components, even if bounded, can be discontinuous across a corner. The modelling of such situations is discussed in detail in Zhang and Mukherjee (1991a). Considering the problem from a physical as well as mathematical point of view, it is seen that the following simple situations lead to continuity of stresses (and bounded Δ) at corners. Such corners are called special corners. Other situations with continuous σ are also possible:

—a right-angled corner with arbitrary applied tractions;
—an acute-angled unloaded corner ($\tau_n^- = \tau_n^- = \tau_s^+ = \tau_s^- = 0$) where $\sigma_{ij} = 0$ (Williams, 1952);
—a corner which arises from using symmetry or zoning in a problem where the point was originally regular or a special corner.

If the stresses are continuous around a corner, the following equations hold from eqn (11):

$$A_{ijk}^- \tau_k^- + B_{ijk}^- \Delta_k^- = A_{ijk}^+ \tau_k^+ + B_{ijk}^+ \Delta_k^+ \quad (i,j,k = 1,2). \tag{18}$$

The above gives three equations, of which at least two are linearly independent. Therefore, the BEM equations (8) plus eqn (18) give enough equations for solving the boundary unknowns including four from each corner.

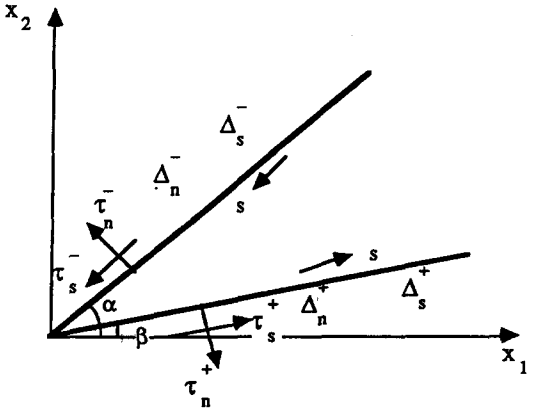

Fig. 1. The elasticity problem at a corner (from Zhang and Mukherjee, 1991a).

This global system is overdetermined since extra equations arise from the stress relations (16). The system, however, has full column rank, is consistent and the number of linearly independent equations equals the number of unknowns. Regular QR decomposition is used to solve this system.

The corresponding sensitivity equations are obtained by differentiating eqn (18) with respect to the design variable **b**. The expression is the following:

$$\overset{\bullet}{A}{}^{-}_{ijk}\tau^{-}_{k} + \overset{\bullet}{B}_{ijk}\Delta^{-}_{k} + A^{-}_{ijk}\overset{\bullet}{\tau}{}^{-}_{k} + B^{-}_{ijk}\overset{\bullet}{\Delta}_{k} = \overset{\bullet}{A}{}^{+}_{ijk}\tau^{+}_{k} + \overset{\bullet}{B}{}^{+}_{ijk}\Delta^{+}_{k} + A^{-}_{ijk}\overset{\bullet}{\tau}{}^{+}_{k} + B^{+}_{ijk}\overset{\bullet}{\Delta}{}^{-}_{k}. \tag{19}$$

These corner sensitivity equations, together with eqn (12), can be used to solve for the unprescribed boundary sensitivities, in a body with special corners.

2.2.4. *Numerical implementation.* The BEM equations (8) (for traction and tangential displacement derivatives) and (12) (for their sensitivities) are discretized in the usual way. The boundary ∂B is subdivided into piecewise quadratic, conforming boundary elements. The variables τ_i and Δ_i are assumed to be piecewise quadratic on these boundary elements. The logarithmically singular kernels are integrated by using log-weighted Gaussian integration. When special corners exist, the corner equations are added to the usual BEM equations, and all the equations are assembled together. The resulting systems are of the form

$$[A]\{\tau\} + [B]\{\Delta\} = \{0\}, \tag{20}$$

$$[A]\{\overset{\bullet}{\tau}\} + [B]\{\overset{\bullet}{\Delta}\} = \{h\} \tag{21}$$

and after switching appropriate columns one obtains, for the unknowns $\{x\}$ and $\{\dot{x}\}$ on the boundary

$$[K]\{x\} = \{r_1\}, \tag{22}$$

$$[K]\{\overset{\bullet}{x}\} = \{r_2\}. \tag{23}$$

Two points deserve mention here. First, the eqns (22) and (23) have the same stiffness matrix $[K]$. The vector $\{r_2\}$ contains the contributions from the second and third lines of eqn (12). Second, eqns (22) and (23) are overdetermined but have full column rank. They have been solved by QR decomposition in the numerical examples that follow (Golub and Van Loan, 1989).

2.2.5. *Numerical results.* Numerical results for two illustrative plane strain problems, from Zhang and Mukherjee (1991a), are described below. The Poisson's ratio υ for these problems is 0.3. The quantities τ, Δ and σ (on ∂B), and their sensitivities, are calculated in each case.

2.2.5.1. The wedge problem. A wedge of angle α subjected to tractions is shown in Fig. 2. These tractions are obtained from the stress function

$$\phi(r, \theta) = Ar^2 \sin 2\theta,$$

with $A = -1/2 \sin(2\alpha)$. In this special problem, the stress tensor $\boldsymbol{\sigma}$ is continuous at the tip of the wedge O (note that here the tractions are functions of α). The wedge angle α is the design variable in this problem. The analytical solution of this problem is

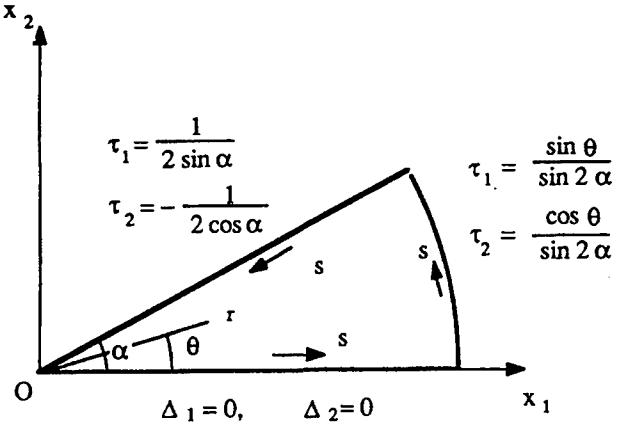

Fig. 2. The wedge problem (from Zhang and Mukherjee, 1991a).

$$\sigma_{11} = \sigma_{22} = 0, \quad \sigma_{12} = 1/\sin 2\alpha,$$

so that

$$\overset{*}{\sigma}_{11} = \overset{*}{\sigma}_{22} = 0, \quad \overset{*}{\sigma}_{12} = \frac{d\sigma_{12}}{d\alpha} = -\frac{2\cos 2\alpha}{\sin^2 2\alpha}.$$

This example provides an opportunity to test the present method for the determination of the stress at the tip of a wedge, and its sensitivity with respect to the wedge angle. In this example (Zhang and Mukherjee, 1991a):

$$\frac{\overset{*}{d}s}{ds} = \frac{1}{\alpha},$$

on the curved surface and $\overset{*}{d}s = 0$ on the straight faces which undergo rigid body rotation.

The numerical results for the stress components and their sensitivities at O are given in Table 1. It is quite remarkable that the numerical result for $\overset{*}{\sigma}_{12}$ captures five significant digits of the analytical solution with only three quadratic boundary elements used to model the boundary ∂B.

2.2.5.2. Elliptical hole in a plate. The classical problem of a planar body with an elliptical hole is considered in this example. Only a quarter of the ellipse needs to be modelled

Table 1. Stress components and their sensitivities at the tip of the wedge (from Zhang and Mukherjee, 1991a)

	σ_{11}	σ_{22}	σ_{12}
Analytical σ_{ij}	0	0	1.1547005
Numerical σ_{ij}	−0.2115977E-5	0.1675500E-6	1.1546976
Error (%)	—	—	0.00025
Analytical σ^*_{ij}	0	0	−1.3333333
Numerical σ^*_{ij}	0.2448821E-4	0.1550109E-4	−1.3333032
Error (%)	—	—	0.0030

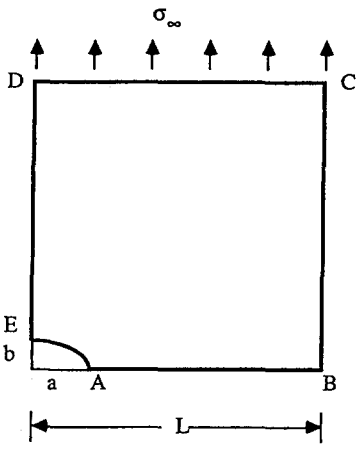

Fig. 3. A body with an elliptical hole (from Zhang and Mukherjee, 1991a).

because of symmetry (Fig. 3). Here, $a = 2$, $b = 1$, $L = 30$, $\sigma_\infty = 1.0$. The corners here arise due to the use of symmetry of the problem. Hence they are special corners where the stresses are continuous. The semi-major axis a is the design variable in this problem. The values of $\overset{*}{d}s/ds$, on the boundary of the body (Fig. 3) are:

$$\text{on } EA: \quad \frac{a\sin^2\theta}{a^2\sin^2\theta + b^2\cos^2\theta}, \quad \text{where: } x_1 = a\cos\theta, \quad x_2 = b\sin\theta,$$

$$\text{on } AB: \quad -1/(L-a), \quad \text{rest zero.}$$

The analytical solution for the tangential "skin" stress and its sensitivity on the ellipse (for an elliptical hole in an infinite plate) are (Barone and Yang, 1989):

$$\sigma_\theta = \sigma_\infty \frac{1+2m-m^2+2m\cos 2\theta}{1+m^2+2\cos 2\theta}$$

$$\overset{*}{\sigma}_\theta = -\sigma_\infty \frac{(1-m)(1+m^2+2m\cos 2\theta)-(m+\cos 2\theta)(1+2m-m^2+2\cos 2\theta)}{(1+m^2+2m\cos 2\theta)^2}\left(\frac{2b}{(a+b)^2}\right),$$

where θ is the eccentric angle and $m = (b-a)/(a+b)$.

The comparisons of analytical and numerical results for σ_θ and $\overset{*}{\sigma}_\theta$ are shown in Figs 4 and 5, respectively. A total of 54 quadratic elements (20 elements are spaced at equal increments of the eccentric angle on the quarter ellipse, 12 elements are applied on AB, 14 on DE, 4 on BC and 4 on CD, respectively) are used for these numerical results. The density of elements on AB and ED is nonuniform, with small elements being placed near the points A and E, respectively. Problems involving stress concentrations are typically sensitive to the mesh around the stress concentration points. The mesh used here is the result of a limited convergence study and previous experience with such problems.

The results from the present method are seen to be very accurate over the entire region. In these figures, the numerical solutions, except for some very small oscillations, essentially agree with the analytical solutions within plotting accuracy. It is remarkable that the computed sensitivity of the stress concentration factor at A is 2.03 and the relative error is 1.54% compared to the analytical result of 2.0.

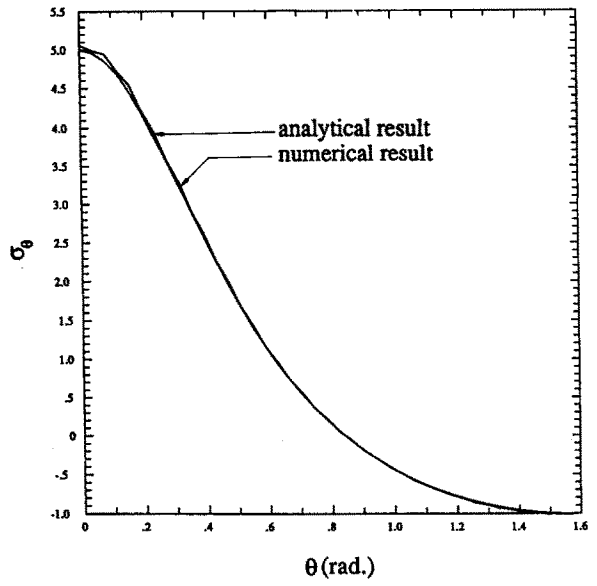

Fig. 4. Angular variation of σ_θ around the quarter ellipse (from Zhang & Mukherjee, 1991a).

3. ELASTOPLASTICITY AND ELASTOVISCOPLASTICITY (MATERIAL NONLINEARITIES)

3.1. *DBEM equations for plane strain*

Following Mukherjee and Chandra (1989) and Zhang *et al.* (1991), the rate form of the DBEM formulation for two-dimensional elastoviscoplasticity (or elastoplasticity) in a simply connected domain is ($i, j, k = 1, 2$)

$$0 = \int_{\partial B} [U_{ij}(\mathbf{b}, P, Q)\dot{\tau}_i(\mathbf{b}, Q) - W_{ij}(\mathbf{b}, P, Q)\dot{\Delta}_i(\mathbf{b}, Q)]\, \mathrm{d}s(\mathbf{b}, Q) + \int_{\partial B} 2GU_{ij,k}(\mathbf{b}, P, q)\dot{\varepsilon}_{ik}^{(n)}(\mathbf{b}, q)\, \mathrm{d}A(\mathbf{b}, q). \quad (24)$$

Here $\dot{\varepsilon}_{ik}^{(n)}$ is the nonelastic strain which must be obtained from a suitable material constitutive

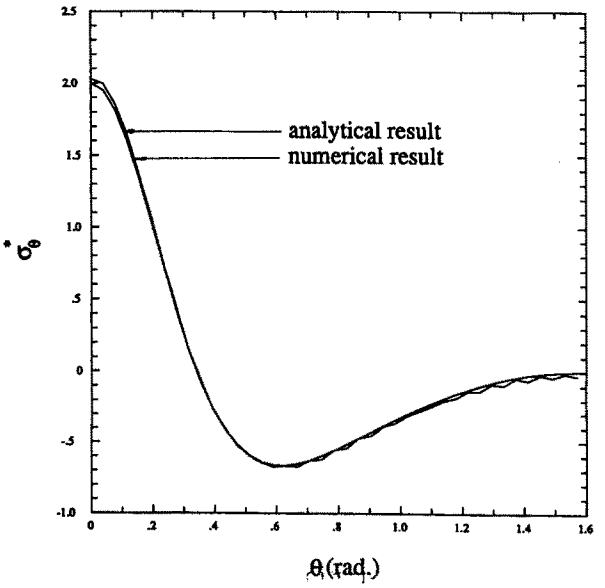

Fig. 5. Angular variation of $\overset{*}{\sigma}_\theta$ around the quarter ellipse (from Zhang and Mukherjee, 1991a).

model. A superposed dot denotes a time derivative (pseudo time derivative for elasto-plasticity). The trace of the nonelastic strain in three dimensions, $\varepsilon_{11}^{(n)}+\varepsilon_{22}^{(n)}+\varepsilon_{33}^{(n)}$, is assumed to vanish, but can be restored, if desired (Mukherjee and Chandra, 1987).

A rate form of the constraint equation (10) is

$$\int_{\partial B} \dot{\Delta}_i \, \mathrm{d}s = \dot{u}_i(B) - \dot{u}_i(A).$$

As can be seen from eqn (24), the rates of the traction and tangential displacement derivative vectors are the primary unknowns on ∂B in this formulation. It can be shown that the rates of stress components at a regular point on ∂B (for plane strain) can be written in terms of the rates of the components of τ, Δ and $\varepsilon^{(n)}$ as: (see Sladek and Sladek, 1986, and Cruse and Vanburen, 1971 for the elastic case) $(i, j, k, l = 1, 2)$

$$\dot{\sigma}_{ij} = A_{ijk}\dot{\tau}_k + B_{ijk}\dot{\Delta}_k + C_{ijkl}\dot{\varepsilon}_{kl}^{(n)} + D_{ij}\dot{\varepsilon}_{kk}^{(n)}, \tag{25}$$

where A_{ijk} and B_{ijk} have been defined before [below eqn (11)] and

$$C_{ijkl} = -c_2 t_i t_j t_k t_l, \quad D_{ij} = \upsilon c_2 t_i t_j,$$

in terms of n_i and t_i, the components of the unit (outward) normal and (anticlockwise) tangent vectors at a point on ∂B. It is important to note here that Δ is now a primary boundary variable and need not be computed by tangential differentiation of the boundary variable and need not be computed by tangential differentiation of the boundary displacement field. Thus, no errors are introduced from tangential differentiation of $\mathbf{u}$ on the boundary, as would be required in a standard BEM formulation. Also, eqn (25) shows that the stress rate is a linear combination of the rates of τ and Δ (assuming that the rate of nonelastic strain is known at time t from a viscoplastic constitutive model) so that the rate of stress on ∂B can be obtained from this formulation with the same accuracy as the rates of τ and Δ. This fact has very important consequences for sensitivity analysis as is discussed later in this chapter (see also, Zhang and Mukherjee, 1991a).

It should be noted that although by assumption, $\dot{\varepsilon}_{11}^{(n)}+\dot{\varepsilon}_{22}^{(n)}+\dot{\varepsilon}_{33}^{(n)} = 0$, $\dot{\varepsilon}_{kk}^{(n)} = \dot{\varepsilon}_{11}^{(n)}+\dot{\varepsilon}_{22}^{(n)}$, in eqn (25), is not equal to zero (see Mukherjee, 1977, for further discussion of this issue).

The nonelastic problem requires that strain and stress rates be obtained at internal points as functions of time. To this end, the version of eqn (24) at an internal source point p is differentiated at that point with respect to the source point coordinates $x_I(p)$. This results in differentiation of the domain integral in eqn (24) whose integrand is already $O(1/r)$ singular. Using the method of Huang and Du (1988), the differentiated domain integral can be transformed to one which is only $O(1/r)$ singular (Mukherjee and Chandra, 1989). The result is

$$\begin{aligned}\dot{u}_{j,I}(\mathbf{b}, p) = &\int_{\partial B} [U_{ij,I}(\mathbf{b}, p, Q)\dot{\tau}_i(\mathbf{b}, Q) - W_{ij,I}(\mathbf{b}, p, Q)\dot{\Delta}_i(\mathbf{b}, Q)] \, \mathrm{d}s(\mathbf{b}, Q) \\ &- 2G\dot{\varepsilon}_{ik}^{(n)}(\mathbf{b}, p) \int_{\partial B} U_{ij,k}(\mathbf{b}, p, Q) n_l(\mathbf{b}, Q) \, \mathrm{d}s(\mathbf{b}, Q) \\ &+ \int_B 2GU_{ij,kI}(\mathbf{b}, p, q)[\dot{\varepsilon}_{ik}^{(n)}(\mathbf{b}, q) - \dot{\varepsilon}_{ik}^{(n)}(\mathbf{b}, p)] \, \mathrm{d}A(\mathbf{b}, q),\end{aligned} \tag{26}$$

with $i, j, k, l = 1, 2$ and $,\bar{I} = \partial/\partial x_I(p)$.

Since $[\dot{\varepsilon}_{ik}^{(n)}(\mathbf{b}, q) - \dot{\varepsilon}_{ik}^{(n)}(\mathbf{b}, p)] \sim O(r)$, the domain integral is now only $1/r$ singular.

Finally, the stress rate components at an internal point can be easily obtained from the components of the velocity gradient and nonelastic strain rate through Hooke's law $(i, j, k = 1, 2)$:

$$\dot{\sigma}_{ij} = \lambda \dot{u}_{k,k}\delta_{ij} + G(\dot{u}_{i,j} + \dot{u}_{j,i}) - 2G\dot{\varepsilon}_{ij}^{(n)}, \tag{27}$$

where $\lambda = 2G\upsilon/(1-2\upsilon)$ is the first Lame constant.

3.2. *DBEM equations for plane stress*

The equations for plane stress are analogous to those for plane strain, but with certain differences. The DBEM equation, corresponding to eqn (24), now has the form (Mukherjee and Chandra, 1987) $(i, j, k = 1, 2)$:

$$\begin{aligned} 0 = \int_{\partial B} [\hat{U}_{ij}(\mathbf{b}, P, Q)\dot{\tau}_i(\mathbf{b}, Q) - \hat{W}_{ij}(\mathbf{b}, P, Q)\dot{\Delta}_i(\mathbf{b}, Q)]\, \mathrm{d}s(\mathbf{b}, Q) \\ + \int_{\partial B} 2G\hat{U}_{ij,k}(\mathbf{b}, P, q)\dot{\varepsilon}_{ik}^{(n)}(\mathbf{b}, q)\, \mathrm{d}A(\mathbf{b}, q) \\ + \int_{\partial B} \hat{\lambda}\hat{U}_{ij,i}(\mathbf{b}, P, q)\dot{\varepsilon}_{kk}^{(n)}(\mathbf{b}, q)\, \mathrm{d}A(\mathbf{b}, q), \end{aligned} \tag{28}$$

where $\hat{U}_{ij}$ and $\hat{W}_{ij}$ have the same forms as U_{ij} and W_{ij} with υ replaced by

$$\hat{\upsilon} = \frac{\upsilon}{(1+\upsilon)}, \quad \text{and with} \quad \hat{\lambda} = \frac{2G\hat{\upsilon}}{(1-2\hat{\upsilon})}.$$

Note that in addition to the usual plane strain–plane stress transformation of υ to $\hat{\upsilon}$, there is also an extra domain integral involving $\dot{\varepsilon}_{11}^{(n)} + \dot{\varepsilon}_{22}^{(n)}$ (see Mukherjee, 1977, 1982).

The stress rate equation at a regular point on ∂B, corresponding to the last term in eqn (25), is $(i, j, k, l = 1, 2)$:

$$\dot{\sigma}_{ij} = \hat{A}_{ijk}\dot{\tau}_k + \hat{B}_{ijk}\dot{\Delta}_k + \hat{C}_{ijkl}\dot{\varepsilon}_{kl}^{(n)}, \tag{29}$$

where, as before, $\hat{\mathbf{A}}$ etc. have the same forms as in eqn (25) with υ replaced by $\hat{\upsilon}$. Note that this time there is no term corresponding to the last term in eqn (25).

The equation at an internal point, corresponding to eqn (26), is $(i, j, k, l = 1, 2)$:

$$\begin{aligned} \dot{u}_{j,I}(\mathbf{b}, p) = \int_{\partial B} [\hat{U}_{ij,I}(\mathbf{b}, p, Q)\dot{\tau}_i(\mathbf{b}, Q) - \hat{W}_{ij,I}(\mathbf{b}, p, Q)\dot{\Delta}_i(\mathbf{b}, Q)]\, \mathrm{d}s(\mathbf{b}, Q) \\ - 2G\dot{\varepsilon}_{ik}^{(n)}(\mathbf{b}, p) \int_{\partial B} \hat{U}_{ij,k}(\mathbf{b}, p, Q)n_l(\mathbf{b}, Q)\, \mathrm{d}s(\mathbf{b}, Q) \\ - \hat{\lambda}\dot{\varepsilon}_{kk}^{(n)}(\mathbf{b}, p) \int_{\partial B} \hat{U}_{ij,i}(\mathbf{b}, p, Q)n_l(\mathbf{b}, Q)\, \mathrm{d}s(\mathbf{b}, Q) \\ + \int_B 2G\hat{U}_{ij,kI}(\mathbf{b}, p, q)[\dot{\varepsilon}_{ik}^{(n)}(\mathbf{b}, q) - \dot{\varepsilon}_{ik}^{(n)}(\mathbf{b}, p)]\, \mathrm{d}A(\mathbf{b}, q) \\ + \int_B \hat{\lambda}\hat{U}_{ij,iI}(\mathbf{b}, p, q)[\dot{\varepsilon}_{kk}^{(n)}(\mathbf{b}, q) - \dot{\varepsilon}_{kk}^{(n)}(\mathbf{b}, p)]\, \mathrm{d}A(\mathbf{b}, q). \end{aligned} \tag{30}$$

Finally, Hooke's law for plane stress, in the presence of nonelastic strains, is $(i, j, k = 1, 2)$:

$$\dot{\sigma}_{ij} = \hat{\lambda}\dot{u}_{k,k}\delta_{ij} + G(\dot{u}_{i,j} + \dot{u}_{j,i}) - 2G\dot{\varepsilon}_{ij^{(n)}} - \hat{\lambda}\dot{\varepsilon}_{kk^{(n)}}\delta_{ij}, \tag{31}$$

which has an extra term compared to eqn (27).

3.3. *Sensitivity equations for plane strain*

The first step here is the differentiation of eqn (24) with respect to a design variable b. Here b is any component of the design vector $\mathbf{b}$. Let a superscribed * denote, as before, the design derivative (with respect to b) of a variable of interest and superscribed ° denote the design derivative of its rate (i.e. $\dot{\sigma}_{ij} = \mathrm{d}\sigma_{ij}/\mathrm{d}b$, $\mathring{\sigma}_{ij} = \mathrm{d}\dot{\sigma}/\mathrm{d}b$). Now one obtains the equations ($i, j, k = 1, 2$)

$$\begin{aligned}
0 = &\int_{\partial B} [U_{ij}(\mathbf{b}, P, Q)\mathring{\tau}_i(\mathbf{b}, Q) - W_{ij}(\mathbf{b}, P, Q)\mathring{\Delta}_i(\mathbf{b}, Q)]\, \mathrm{d}s(\mathbf{b}, Q) \\
&+ \int_{\partial B} [\overset{*}{U}_{ij}(\mathbf{b}, P, Q)\dot{\tau}_i(\mathbf{b}, Q) - \overset{*}{W}_{ij}(\mathbf{b}, P, Q)\dot{\Delta}_i(\mathbf{b}, Q)]\, \mathrm{d}s(\mathbf{b}, Q) \\
&+ \int_{\partial B} [U_{ij}(\mathbf{b}, P, Q)\dot{\tau}_i(\mathbf{b}, Q) - W_{ij}(\mathbf{b}, P, Q)\dot{\Delta}_i(\mathbf{b}, Q)]\, \overset{*}{\mathrm{d}}s(\mathbf{b}, Q) \\
&+ \int_{\partial B} 2GV_{ijk}(\mathbf{b}, P, q)\mathring{\varepsilon}_{ik^{(n)}}(\mathbf{b}, q)\, \mathrm{d}A(\mathbf{b}, q) \\
&+ \int_{\partial B} 2G\overset{*}{V}_{ijk}(\mathbf{b}, P, q)\dot{\varepsilon}_{ik^{(n)}}(\mathbf{b}, q)\, \mathrm{d}A(\mathbf{b}, q) \\
&+ \int_{\partial B} 2GV_{ijk}(\mathbf{b}, P, q)\dot{\varepsilon}_{ik^{(n)}}(\mathbf{b}, q)\, \overset{*}{\mathrm{d}}A(\mathbf{b}, q),
\end{aligned} \tag{32}$$

where $V_{ijk} = U_{ij,k}$. At the start of a time step, half of the sensitivities of the rates of Δ_i and τ_i are to be determined, while the rest of the quantities in eqn (32) are known. This is because the rates of τ_i, Δ_i and $\varepsilon_{ij^{(n)}}$ are known from a solution of the usual DBEM problem up to this time, and the sensitivity of the nonelastic strain rate is known from differentiating a suitable constitutive model. A discussion of viscoplastic constitutive models appears later in this chapter.

The new quantity above:

$$\overset{*}{\mathrm{d}}A = \overset{*}{x}_{k,k}(q)\, \mathrm{d}A. \tag{33}$$

While the quantity $\overset{*}{x}_i(P)$, which is the rate of change of a coordinate of a boundary point with respect to a design variable b, is relatively easy to compute from eqn (15), such is not the case for $\overset{*}{x}_i(p)$. The internal points must move in a manner compatible with the boundary motion, but this motion is not unique and additional assumptions are necessary to tie the motion of internal points in B to the motion of the boundary ∂B. Also, dependent variables such as stress or displacement can depend on b in an explicit as well as in an implicit manner through $\overset{*}{x}_i(p)$. Thus, for example, the stress field inside a hollow disc subjected to external pressure is a function of its position as well as the disc radii a and b. Here, radius b could be a design variable. A consequence of this fact is that for a dependent variable $\chi(\mathbf{x}(p), b)$, one gets a material derivative

$$\overset{*}{\chi}(x_i(p), b) = \left.\frac{\partial \chi}{\partial b}\right|_{x_i(p)} + \frac{\partial \chi}{\partial x_i(p)} \overset{*}{x}_i(p).$$

Obviously, an assumption regarding the design velocity at an internal point will affect the value $\overset{*}{\chi}$.

The sensitivity equation for the stress rate at a boundary point, corresponding to eqn (25), becomes $(i, j, k, l = 1, 2)$:

$$\mathring{\sigma}_{ij} = A_{ijk}\mathring{\tau}_k + B_{ijk}\mathring{\Delta}_k + C_{ijkl}\mathring{\varepsilon}_{kl^{(n)}} + D_{ij}\mathring{\varepsilon}_{kk^{(n)}} + \overset{*}{A}_{ijk}\dot{\tau}_k + \overset{*}{B}_{ijk}\dot{\Delta}_k + \overset{*}{C}_{ijkl}\dot{\varepsilon}_{kl^{(n)}} + \overset{*}{D}_{ij}\dot{\varepsilon}_{kk^{(n)}} \tag{34}$$

which expresses $\mathring{\sigma}_{ij}$ as a linear combination of $\dot{\tau}_i$, $\dot{\Delta}_i$, $\dot{\varepsilon}_{ij^{(n)}}$ and their sensitivities. Hence, one expects to obtain $\mathring{\sigma}_{ij}$ as accurately as $\mathring{\tau}_i$ and $\mathring{\Delta}_i$.

Finally, one must derive an equation for the sensitivities of the velocity gradients at an internal point. The resulting equation has the form (all indices 1, 2):

$$\begin{aligned}
\mathring{u}_{j,I}(\mathbf{b}, p) = &\int_{\partial B} [V_{ijI}(\mathbf{b}, p, Q)\mathring{\tau}_i(\mathbf{b}, Q) - Y_{ijI}(\mathbf{b}, p, Q)\mathring{\Delta}_i(\mathbf{b}, Q)]\, \mathrm{d}s(\mathbf{b}, Q) \\
&+ \int_{\partial B} [\overset{*}{V}_{ijI}(\mathbf{b}, p, Q)\dot{\tau}_i(\mathbf{b}, Q) - \overset{*}{Y}_{ijI}(\mathbf{b}, p, Q)\dot{\Delta}_i(\mathbf{b}, Q)]\, \mathrm{d}s(\mathbf{b}, Q) \\
&+ \int_{\partial B} [V_{ijI}(\mathbf{b}, p, Q)\dot{\tau}_i(\mathbf{b}, Q) - Y_{ijI}(\mathbf{b}, p, Q)\dot{\Delta}_i(\mathbf{b}, Q)]\, \overset{*}{\mathrm{d}}s(\mathbf{b}, Q) \\
&- 2G\mathring{\varepsilon}_{ik^{(n)}}(\mathbf{b}, p) \int_{\partial B} V_{ijk}(\mathbf{b}, p, Q) n_l(\mathbf{b}, Q)\, \mathrm{d}s(\mathbf{b}, Q) \\
&- 2G\dot{\varepsilon}_{ik^{(n)}}(\mathbf{b}, p) \int_{\partial B} \overset{*}{V}_{ijk}(\mathbf{b}, p, Q) n_l(\mathbf{b}, Q)\, \mathrm{d}s(\mathbf{b}, Q) \\
&- 2G\dot{\varepsilon}_{ik^{(n)}}(\mathbf{b}, p) \int_{\partial B} V_{ijk}(\mathbf{b}, p, Q) \overset{*}{n}_l(\mathbf{b}, Q)\, \mathrm{d}s(\mathbf{b}, Q) \\
&- 2G\dot{\varepsilon}_{ik^{(n)}}(\mathbf{b}, p) \int_{\partial B} V_{ijk}(\mathbf{b}, p, Q) n_l(\mathbf{b}, Q)\, \overset{*}{\mathrm{d}}s(\mathbf{b}, Q) \\
&+ \int_B 2GP_{ijkI}(\mathbf{b}, p, q)[\mathring{\varepsilon}_{ik^{(n)}}(\mathbf{b}, q) - \mathring{\varepsilon}_{ik^{(n)}}(\mathbf{b}, p)]\, \mathrm{d}A(\mathbf{b}, q) \\
&+ \int_B 2G\overset{*}{P}_{ijkI}(\mathbf{b}, p, q)[\dot{\varepsilon}_{ik^{(n)}}(\mathbf{b}, q) - \dot{\varepsilon}_{ik^{(n)}}(\mathbf{b}, p)]\, \mathrm{d}A(\mathbf{b}, q) \\
&+ \int_B 2GP_{ijkI}(\mathbf{b}, p, q)[\dot{\varepsilon}_{ik^{(n)}}(\mathbf{b}, q) - \dot{\varepsilon}_{ik^{(n)}}(\mathbf{b}, p)]\, \overset{*}{\mathrm{d}}A(\mathbf{b}, q),
\end{aligned} \tag{35}$$

where $Y_{ijk} = W_{ij,k}$ and $P_{ijkl} = U_{ij,kl}$.

Although this equation is long, the entire right-hand side of it is known at this stage so that the required sensitivity of the velocity gradient at an internal point, $\mathring{u}_{j,I}$, can be obtained by a series of function evaluations. The boundary kernels are regular and the domain integrands are $1/r$ singular. These domain integrals must be determined very accurately. The $1/r$ weighted Gaussian integration formulae from Cristescu and Loubignac (1978) or Pina *et al.* (1981), for example, were not sufficiently accurate for the purpose of this work. The mapping method described in Mukherjee (1982, pp. 91–92) has been adopted here.

There stress rate sensitivities, at an internal point, are obtained from a differentiated version of Hooke's law [eqn (27)].

Analogous sensitivity equations for plane stress can be easily derived.

3.4. *Modelling of corners for plane strain*

The modelling of corners for elastoplastic and elastoviscoplastic problems follows the same ideas as those described earlier for elasticity problems.

If stress components are continuous across a corner, the following equations (for plane strain) follow from eqn (25) ($i, j, k, l = 1, 2$):

$$A^-_{ijk}\dot{\tau}^-_k + B^-_{ijk}\dot{\Delta}^-_k + C^-_{ijkl}\dot{\varepsilon}_{kl^{(n)}} + D^-_{ij}\,\dot{\varepsilon}_{kk^{(n)}} = A^+_{ijk}\dot{\tau}^+_k + B^+_{ijk}\dot{\Delta}^+_k + C^+_{ijkl}\dot{\varepsilon}_{kl^{(n)}} + D^+_{ij}\,\dot{\varepsilon}_{kk^{(n)}}. \tag{36}$$

The superscripts $-$ and $+$ denote, as before, quantities before and after the corner in a counterclockwise direction (Fig. 1). Since the stress, by assumption, is continuous across a corner so is the nonelastic strain rate. Also, the rate of nonelastic strain is known at any time once the stress (and state variables, if any) are known at a corner at this time. (A discussion of viscoplastic constitutive models appears next in this chapter.) Thus, eqns (36) are three linearly independent scalar equations relating the rates of τ_i and Δ_i before and after the corner. At least two of these equations are linearly independent. Thus, the DBEM eqns (24) plus eqns (36) give enough equations for determining all the boundary unknowns including four from each corner.

The global system is overdetermined since extra equations arise from the stress relation (3). The system, however, has full column rank, is consistent and the number of linearly independent equations equals the number of unknowns. Regular QR decomposition is used to solve this system (Golub and Van Loan, 1989).

The sensitivity equation at a corner, across which σ_{ij} and $\overset{*}{\sigma}_{ij}$ are continuous, has the form:

$$\begin{aligned} &A^-_{ijk}\mathring{\tau}^-_k + B^-_{ijk}\mathring{\Delta}^-_k + C^-_{ijkl}\mathring{\varepsilon}_{kl^{(n)}} + D^-_{ij}\,\mathring{\varepsilon}_{kk^{(n)}} + \overset{*}{A}{}^-_{ijk}\dot{\tau}^-_k + \overset{*}{B}{}^-_{ijk}\dot{\Delta}^-_k + \overset{*}{C}{}^-_{ijkl}\dot{\varepsilon}_{kl^{(n)}} + \overset{*}{D}{}^-_{ij}\,\dot{\varepsilon}_{kk^{(n)}} \\ &\quad = A^+_{ijk}\mathring{\tau}^+_k + B^+_{ijk}\mathring{\Delta}^+_k + C^+_{ijkl}\mathring{\varepsilon}_{kl^{(n)}} + D^+_{ij}\,\mathring{\varepsilon}_{kk^{(n)}} + \overset{*}{A}{}^+_{ijk}\dot{\tau}^+_k + \overset{*}{B}{}^+_{ijk}\dot{\Delta}^+_k + \overset{*}{C}{}^+_{ijkl}\dot{\varepsilon}_{kl^{(n)}} + \overset{*}{D}{}^+_{ij}\,\dot{\varepsilon}_{kk^{(n)}}. \end{aligned} \tag{37}$$

The corresponding sensitivity equations for plane stress problems can be obtained in an entirely analogous fashion, and are not repeated here.

3.5. *Viscoplastic constitutive model*

As has been mentioned earlier, viscoplastic constitutive equations are needed to determine $\dot{\varepsilon}_{ij^{(n)}}$ and its sensitivity, $\mathring{\varepsilon}_{ij^{(n)}}$, as functions of time, Mukherjee's book (Mukherjee, 1982) has a discussion of such unified models with state variables. A general form of such a law is ($i, j = 1, 2, k = 1, 2, \ldots, m$)

$$\dot{\varepsilon}_{ij^{(n)}} = f_{ij}(\sigma_{ij}, q_{ij^{(k)}}) \quad \text{and} \quad \dot{q}_{ij^{(k)}} = g_{ij^{(k)}}(\sigma_{ij}, q_{ij^{(n)}}), \tag{38}$$

where $q_{ij^{(k)}}$ are suitably defined state variables, which can be scalars or tensors.

Differentiating eqn (38) with respect to a design variable b gives $\mathring{\varepsilon}_{ij^{(n)}}$ and $\mathring{q}_{ij^{(k)}}$ in terms of the sensitivities of the stress and state variables:

$$\mathring{\varepsilon}_{ij^{(n)}} = \frac{\partial f_{ij}}{\partial \sigma_{ml}}\overset{*}{\sigma}_{ml} + \frac{\partial f_{ij}}{\partial q_{ml^{(k)}}}\overset{*}{q}_{ml^{(k)}}$$

and

$$\mathring{q}_{ij^{(k)}} = \frac{\partial g_{ij^{(k)}}}{\partial \sigma_{ml}} \overset{*}{\sigma}_{ml^+} \frac{\partial g_{ij^{(k)}}}{\partial q_{ml^{(p)}}} \overset{*}{q}_{ml^{(p)}}. \tag{39}$$

Constitutive equations for small strain elastoplasticity are available in many standard books, and are not repeated here.

3.6. *Numerical implementation*

3.6.1. *Discretization of equations.* For plane strain problems, the DBEM equations (24) and (26), and the sensitivity equations (32) and (35), are discretized in the usual way. (Of course, corresponding equations must be used for plane stress problems.) The boundary ∂B is subdivided into piecewise quadratic, conforming boundary elements. The variables $\dot{\tau}_i$, $\dot{\Delta}_i$ and their sensitivities are assumed to be piecewise quadratic on the boundary elements. The domain of the body is divided into $Q4$ internal cell elements. The nonelastic strain rate components, $\dot{\varepsilon}_{ij^{(n)}}$, and the sensitivities, as well as the quantity $\overset{*}{\mathrm{d}A}/\mathrm{d}A$, are interpolated on the $Q4$ internal cells.

As has been mentioned before, singular integrals must be evaluated with great care for these problems. Logarithmically singular integrands are integrated with log-weighted Gaussian integration formulae on the boundary elements. The $1/r$ singular domain integrals are first transformed into regular ones by mapping (Mukherjee, 1982, pp. 91–92) and then evaluated by regular Gaussian quadrature on a square. The number of Gauss points used for regular and log-singular boundary integrals are 20 and 16, respectively. For regular domain integrals, as well as $1/r$ singular domain integrals which are transformed to regular form, the number of Gauss points used is 3×3.

When corners exist on ∂B, the corner equations are added to the usual DBEM equations, and all the equations are assembled together. The resulting systems of boundary equations are of the form:

$$[A]\{\dot{\Delta}\} + [B]\{\dot{\tau}\} = \{C_1\}, \tag{40}$$

$$[A]\{\mathring{\Delta}\} + [B]\{\mathring{\tau}\} = \{C_2\}, \tag{41}$$

where the right hand sides of eqns (40) and (41) contain the nonelastic strain rates. The vector $\{C_2\}$, however, contains rates of $\dot{\tau}_i$ and $\dot{\Delta}_i$ as well as $\dot{\varepsilon}_{ij^{(n)}}$ and $\mathring{\varepsilon}_{ij^{(n)}}$ [see eqn (32)]. It is very important to note that $\{C_1\}$ and $\{C_2\}$ are known at any time during a time-matching procedure, and that the coefficient matrices $[A]$ and $[B]$ are identical in the two equations above. The usual switching of columns leads to equations of the type

$$[K]\{\dot{x}\} = \{r_1\}, \tag{42}$$

$$[K]\{\mathring{x}\} = \{r_2\}, \tag{43}$$

for the unknowns $\{\dot{x}\}$ and $\{\mathring{x}\}$ on ∂B. The matrix $[K]$ is rectangular in the presence of corners. Equations (42) and (43) are solved using regular QR decomposition (Golub and Van Loan, 1989).

3.6.2. *Solution strategy.* The solution algorithm for the standard elastoviscoplastic problem, which involves solutions of appropriate equations at the beginning of each time step and then marching forward in time, has been used by several researchers (e.g. Mukherjee, 1982). The sensitivity calculations must also be carried out using an analogous procedure, in parallel with the standard calculations. The algorithm is described below.

The elastic DBEM equations are solved at zero time to obtain the quantities of interest, τ_i, Δ_i and σ_{ij}, and their sensitivities. The constitutive equations (38) and (39) are used to

obtain $\dot{\varepsilon}_{ij^{(n)}}$, $\dot{q}_{ij^{(k)}}$, $\mathring{\varepsilon}_{ij^{(n)}}$ and $\mathring{q}_{ij^{(k)}}$. The initial value of the state variable (s) is specified and its initial sensitivity is zero.

Figure 6 illustrates the procedure for moving to $t+\Delta t$ when the solution up to time t is known. The DBEM equation (24) and the corresponding sensitivity equation (32) are first solved in order to obtain the unprescribed values of $\dot{\tau}_i$, $\dot{\Delta}_i$, $\mathring{\tau}_i$ and $\mathring{\Delta}_i$ on ∂B. Now the algebraic boundary equations (25) and (34) and Hooke's law are used to obtain $\dot{\sigma}_{ij}$, $\dot{\varepsilon}_{ij}$, $\mathring{\sigma}_{ij}$ and $\mathring{\varepsilon}_{ij}$ on ∂B. Next, the internal integral equations (26) and (35), together with Hooke's law, are used to obtain $\dot{\sigma}_{ij}$, $\dot{\varepsilon}_{ij}$, $\mathring{\sigma}_{ij}$ and $\mathring{\varepsilon}_{ij}$ at selected internal points. The rates are integrated to obtain the quantities σ_{ij}, ε_{ij} and $q_{ij^{(k)}}$ and their sensitivities $\overset{*}{\sigma}_{ij}$, $\overset{*}{\varepsilon}_{ij}$, $\overset{*}{q}_{ij^{(k)}}$ at time $t+\Delta t$. The constitutive equations (38) and (39) are now used to calculate $\dot{\varepsilon}_{ij^{(n)}}$, $\dot{q}_{ij^{(k)}}$, $\mathring{\varepsilon}_{ij^{(n)}}$ and $\mathring{q}_{ij^{(k)}}$ at $t+\Delta t$.

Corner equations, if present, must be assembled together with the DBEM and sensitivity equations (24) and (26) at each time. The displacement sensitivities, if desired, can be obtained from the equation:

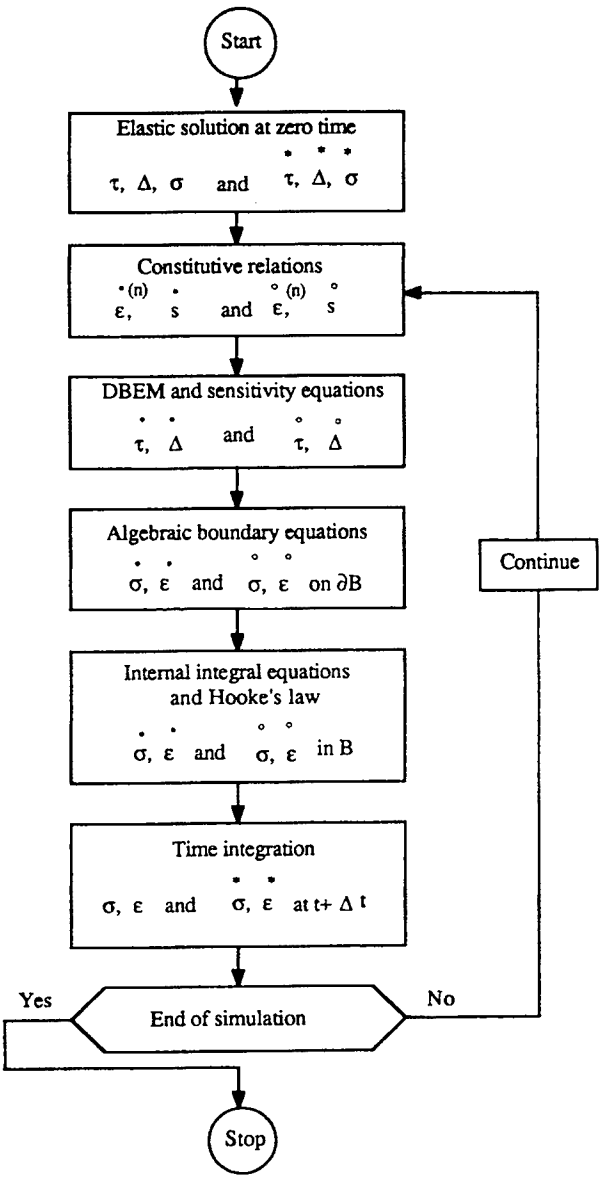

Fig. 6. Solution strategy for elastoviscoplastic problems (from Zhang *et al.*, 1991).

$$\overset{*}{\mathbf{u}}(P) = \overset{*}{\mathbf{u}}(P_0) + \int_{P_0}^{P} \overset{*}{\Delta}\, \mathrm{d}s + \int_{P_0}^{P} \Delta\, \mathrm{d}\overset{*}{s}, \tag{44}$$

where P_0 is a point on ∂B where $\overset{*}{u}_i$ is known and P is any other point of interest on ∂B.

Time integration has been carried out with fixed, small time steps ($\Delta t = 0.01$ s). A variable step explicit time integration scheme, with automatic time step control, will soon be implemented. (See Mukherjee, 1982, for a discussion of time integration schemes for unified viscoplastic models.)

Classical elastoplastic problems can also be solved by using a small variation of this algorithm. Now the constitutive model includes a dependence of $\overset{*}{\dot{\varepsilon}}_{ij}^{(n)}$ on $\overset{*}{\sigma}_{ij}$ as well as on the stress components and their sensitivities. The situation becomes analogous to the solution of classical elastoplastic problems by the BEM in that iterations must now be carried out within each time step. The sensitivity problem, however, still has approximately the same level of complexity as the original elastoplastic problem. Also, many of the matrices and solution procedures from the original elastoplastic problem can still be used for solving the sensitivity problem.

3.7. *Numerical results*

3.7.1. *Illustrative constitutive model.* The DBEM formulation presented in this chapter is quite general and any of a large number of elastoviscoplastic constitutive models can be used here to describe material behavior. The reader is referred to Mukherjee's book (Mukherjee, 1982) for a discussion of such models.

The particular model chosen for the numerical results discussed in this paper is due to Anand (1982). This is a unified elastoviscoplastic model with a single scalar internal variable. The model, adapted to the present multiaxial situation, is described by the equations:

$$\dot{\varepsilon}_{ij}^{(n)} = \frac{3\dot{\varepsilon}^{(n)}}{2\sigma}\sigma'_{ij}, \tag{45}$$

where σ'_{ij} are the components of the deviatoric part of the Cauchy stress and σ is the stress invariant defined as:

$$\sigma = \sqrt{\tfrac{3}{2}\sigma'_{ij}\sigma'_{ij}}.$$

The invariant $\dot{\varepsilon}^{(n)}$ is given by the equation

$$\dot{\varepsilon}^{(n)} = A\, \mathrm{e}^{-Q/\mathrm{K}T}\left(\frac{\sigma}{s}\right)^{1/m}, \tag{46}$$

together with the evolution equations

$$\dot{s} = h_0\left(1 - \frac{s}{s_c}\right)\dot{\varepsilon}^{(n)}, \tag{47}$$

where

$$s_c = s_a\left[\frac{\dot{\varepsilon}^{(n)}}{A}\mathrm{e}^{Q/\mathrm{K}T}\right]^n.$$

Here T is the temperature in degrees Kelvin, Q is the activation energy and K is the Boltzmann constant. Also A, h_0, s_a, m and n are material constants of which m and n are, in general, temperature dependent. The particular parameters used here are representative of F_e—0.05 carbon steel in a temperature range of 1173–1573 K and strain rate range of

$1.4 \times 10^{-4}\ s^{-1}$ to $2.3 \times 10^{-2}\ s^{-1}$. These parameters have been used for all the isothermal simulations (at $T = 1173$ K) reported here. They are:

$$A = 10^{11}\ s^{-1} \qquad h_0 = 1329.22\ \text{MPa}$$
$$s = 147.6\ \text{MPa} \qquad m = 0.147$$
$$n = 0.03 \qquad Q/\text{K} = 3.28 \times 10^4\ \text{K},$$

together with elastic constants (at 1173 K)

$$G = 2.2615 \times 10^3\ \text{MPa} \qquad \upsilon = 0.3.$$

Also, the initial value of the state variables is taken to be 47.11 MPa.

3.7.2. *Numerical examples.* A computer program for numerically calculating sensitivities for general two-dimensional (plane strain or plane stress) elastoviscoplastic problems has been developed. It is crucial that such a program, for history dependent sensitivities for nonlinear problems, be carefully checked against analytical solutions for simple geometrical situations. Such tests for one-dimensional strain of a square (one-dimensional strain and one-dimensional stress) and pressurization of a thin disc (plane stress) have been completed, and are described below.

3.7.2.1. One-dimensional strain of a square. The physical situation as well as the results are shown in Figs 7 and 8. Figure 7 shows a one-dimensional strain problem in which the only nonzero displacement is u_1, while Fig. 8 depicts a one-dimensional stress problem with the only nonzero stress σ_{11}. Of course, the plane strain version of the two-dimensional DBEM computer program is employed to solve the one-dimensional strain problem while the plane stress version is used to solve the one-dimensional stress problem. In both cases, a constant velocity $v_0 = 2 \times 10^{-3}\ \text{m s}^{-1}$ is applied in the x_1 direction (on the right vertical plane of the square) with a very small value of initial strain in this direction. The design

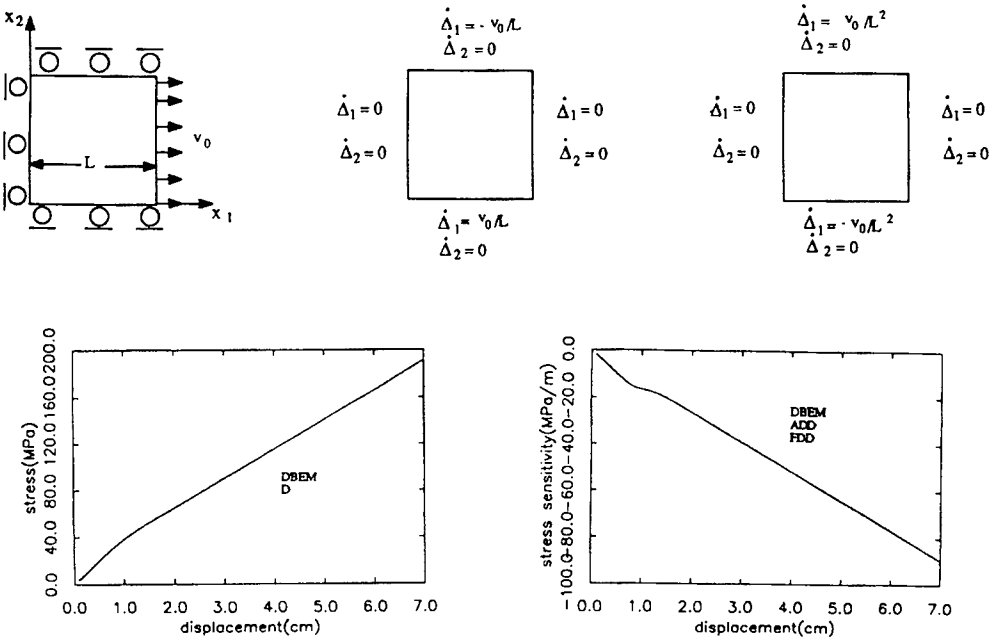

Fig. 7. Results for one-dimensional strain. $v_0 = 2 \times 10^{-3}$ (m s^{-1}). FDD: finite difference of direct solutions, D: direct, DBEM: derivative BEM, ADD: analytical differentiation of direct solutions (from Zhang *et al.*, 1991).

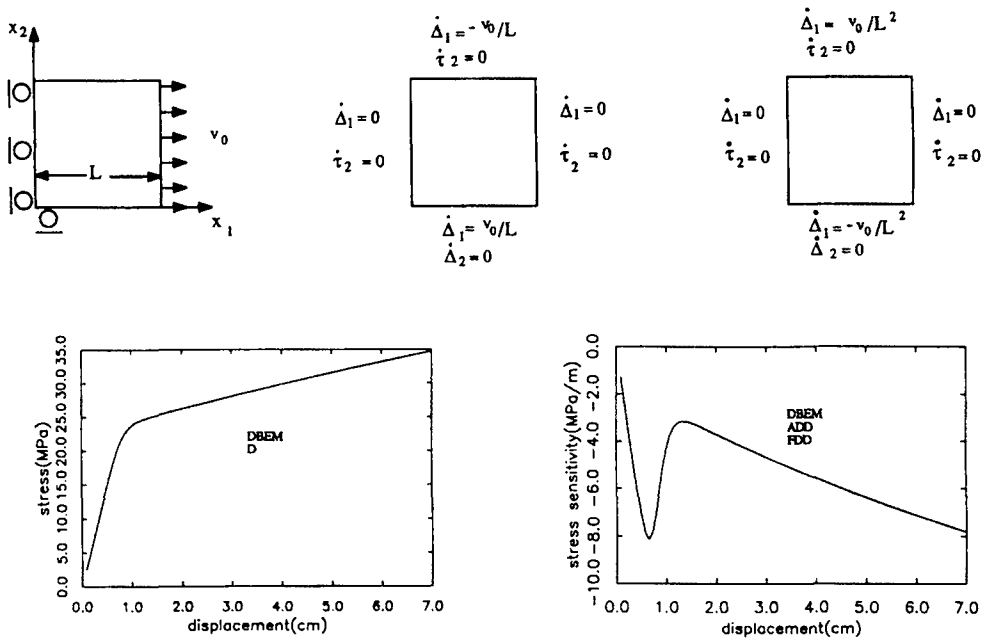

Fig. 8. Results for one-dimensional stress. $v_0 = 2 \times 10^{-3}$ (m s^{-1}). FDD: finite difference of direct solutions, D: direct, DBEM: derivative BEM, ADD: analytical differentiation of direct solutions (from Zhang *et al.*, 1991).

variable is the initial length of the square, L, in the x_1 direction. Here, $\dot{ds}/ds = 1/L$ and $\dot{dA}/dA = 1/L$. The dimensions of the square are 2 m × 2 m. The constant time step Δt, for explicit time integration, is 0.01s.

The modelling of the boundaries of the square, in terms of the rates of Δ and τ and their sensitivities, also appears in Figs 7 and 8. The DBEM has nonstandard boundary variables and these must be prescribed such that a unique solution is obtained. Information can be lost if a zero Δ_i is prescribed on part of a boundary instead of a constant u_i. This can be remedied by using constraint equations [see the equation following (24)]. Such constraint equations are recommended in general. Here, for a simple geometrical situation, $\dot{\Delta}_s$ is prescribed on certain boundaries of the square.

Another concern, of course, is rigid body motion. This DBEM formulation gives unique results which are unaffected by rigid body translations, as long as Δ, τ, σ and ε are sought. Of course, calculation of displacements requires specification of the displacement of some point in the structure. An imposed rigid body rotation, however, changes the values of Δ_n on ∂B, without changing the stresses in the body. Thus, rigid body rotations must be eliminated by the boundary conditions in order to get a unique solution from the DBEM equations.

In summary, a DBEM model, plus a prescribed displacement at one point in the body, must be consistent with a corresponding usual BEM model in terms of $\mathbf{u}$ and τ on ∂B.

Figure 7 shows the stress–displacement plot in the x_1 direction (σ_{11} as a function of u_1) and the corresponding sensitivity plot ($\dot{\sigma}_{11}$ vs u_1) for the one-dimensional strain problem. The displacement is the abscissa since, in these examples, the velocity, rather than the strain rate, is constant. Here "D" refers to the direct solution, "FDD" to the finite difference of direct solutions and "ADD" to the analytical differentiation of a direct solution. The direct is a time-marching solution obtained by integrating the one-dimensional equations with an explicit integration scheme. It can be essentially regarded as the exact solution of the problem. The FDD solution is obtained with $\Delta L = 0.001$. The various solutions are seen to agree perfectly within plotting accuracy.

The stress–displacement plot shows the characteristic nearly bilinear behavior of an elastoviscoplastic constitutive model. The ratio of elastic to plastic slopes, in this plot, is

considerably less than, say, uniaxial plots in Anand (1982) because this is a one-dimensional strain problem but σ_{11} is plotted here. The stress invariant σ, from eqn (45), is considerably less than σ_{11}. (The value of σ, at $u = 7$ cm, is 29.51 MPa.) The corresponding sensitivity plot in Fig. 7 shows negative sensitivity throughout with a kink in the curve around the transition region where significant viscoplastic deformation sets in.

The corresponding situation for the one-dimensional stress problem is depicted in Fig. 8. Two points should be noted here. The first is that the ratio of elastic to plastic slopes now corresponds to that seen in usual one-dimensional stress–strain plots (e.g. Anand, 1982) since σ_{11} is now the only stress and the stress invariant σ equals σ_{11}. Second, the corresponding sensitivity plot is now considerably more complicated than the one-dimensional strain case, especially in the elastoviscoplastic transition region.

In order to understand the nature of the sensitivity plot in the one-dimensional stress case (Fig. 8), stress–displacement plots for two values of length ($L = 2$ m and $L = 2.5$ m) are shown in Fig. 9. It is seen that in the elastic region $\mathring{\sigma}_{11} = -Ev_0/L^2$ ($\mathring{\sigma}_{11}$ is the slope of the $\overset{*}{\sigma}_{11}$ curve in Fig. 8) and in the fully developed plastic region $\mathring{\sigma}_{11} \approx -E_T v_0/L^2$ in terms of the tangent modulus E_T which is, of course, less than E. The transition displacement, however, is also a function of L ($u_Y = L\sigma_Y/E$ for an idealized elastoplastic model with a yield stress σ_Y). This causes shifting of the curve for $L = 2.5$ m, relative to that for $L = 2$ m. Consequently, the two curves come closer together in the transition region, leading to a positive value of $\mathring{\sigma}_{11}$ in this region. Figure 10 shows a schematic figure to illustrate this effect for ideal elastoplasticity.

3.7.2.2. Pressurization of a disc. The next example is that of a thin annular disc (plane stress) subjected to external pressure p_0 increasing at a constant rate. A quarter of the disc is shown in Fig. 11. The internal radius a is the design variable. The values of $\overset{*}{\mathrm{d}}s/\mathrm{d}s$ in this problem are: on DA: $1/a$, on AB and CS: $-1/(b-a)$, rest zero. The value of $\overset{*}{\mathrm{d}}A/\mathrm{d}A$ is $-2/(b-a)$.

The boundary mesh consists of five quadratic elements on each of the four segments AB, BC, CD and DA in Fig. 11. On a given segment, the boundary elements are of equal length. The internal mesh is regular, with equal increments in length along a radius and equal increments in θ along a quarter circle centered at O. Here, a 10×10 grid of 100 $Q4$ internal cells is used. All the internal cells have straight sides, but cells with curved sides can be generated, if desired. It is clear that in this mesh the internal nodes on ∂B coincide with all the boundary (including midside) nodes.

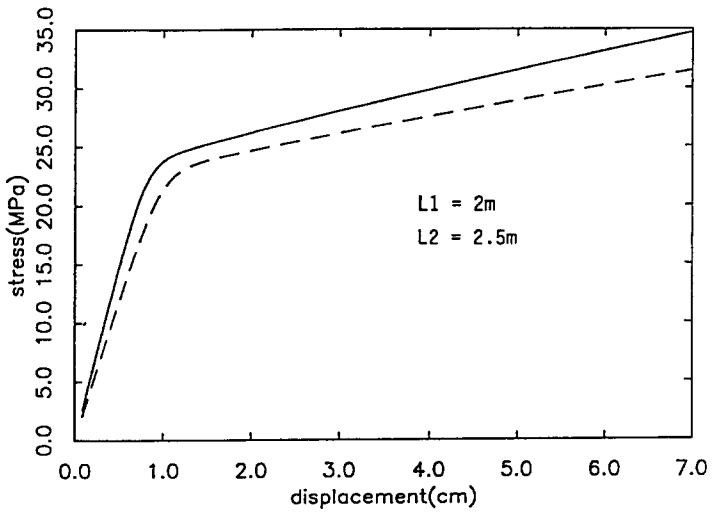

Fig. 9. Stress for the one-dimensional stress problem, for two different values of the length of the square. Solutions from the direct method (from Zhang *et al.*, 1991).

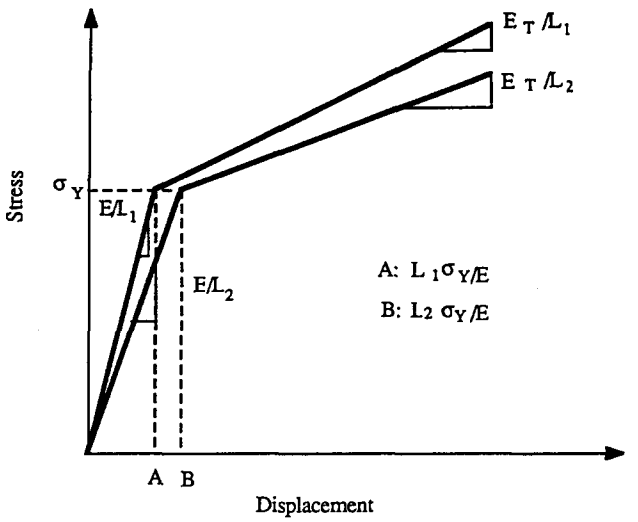

Fig. 10. Schematic diagram for ideal elastoplasticity, for two specimens of initial lengths L_1 and L_2, respectively (from Zhang *et al.*, 1991).

In the numerical examples, $a = 1$ m, $b = 1.5$ m, the rate of $p_0 = 5$ MPa s^{-1} and Δt, for explicit time integration with fixed time steps, is 0.1 s.

Before discussing the DBEM results, it is useful to say something about the direct solution of the problem that has been used for comparison with the DBEM solution. Using standard mechanics for this cylindrical geometry, it can be shown that (Mukherjee, 1979, 1982), for plane stress ($\dot{\sigma}_{zz} = 0$),

$$\dot{\sigma}_{rr}(r,t) = \frac{E}{2}\left[\int_a^r \frac{\dot{\varepsilon}_{rr}^{(n)} - \dot{\varepsilon}_{\theta\theta}^{(n)}}{\rho}\,d\rho - \frac{(r^2-a^2)}{(b^2-a^2)}\frac{b^2}{r^2}\int_a^b \frac{\dot{\varepsilon}_{rr}^{(n)} - \dot{\varepsilon}_{\theta\theta}^{(n)}}{\rho}\,d\rho\right]$$

$$+\frac{E}{2}\frac{1}{r^2}\left[\int_a^r \rho\dot{\varepsilon}_{zz}^{(n)}\,d\rho - \frac{(r^2-a^2)}{(b^2-a^2)}\int_a^b \rho\dot{\varepsilon}_{zz}^{(n)}\,d\rho\right]$$

$$-\dot{p}_i\frac{(b^2-r^2)}{(b^2-a^2)}\frac{a^2}{r^2} - \dot{p}_0\frac{(r^2-a^2)}{(b^2-a^2)}\frac{b^2}{r^2}, \quad (48)$$

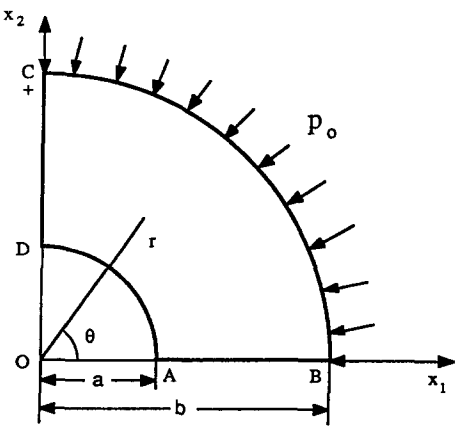

Fig. 11. Quarter of hollow disc in plane stress (from Zhang *et al.*, 1991).

$$\dot{\sigma}_{\theta\theta}(r,t) = \frac{E}{2}\left[\int_a^r \frac{\dot{\varepsilon}_{rr^{(n)}} - \dot{\varepsilon}_{\theta\theta^{(n)}}}{\rho}\,d\rho - \frac{(r^2+a^2)}{(b^2-a^2)}\frac{b^2}{r^2}\int_a^b \frac{\dot{\varepsilon}_{rr^{(n)}} - \dot{\varepsilon}_{\theta\theta^{(n)}}}{\rho}\,d\rho\right]$$
$$-\frac{E}{2}\frac{1}{r^2}\left[\int_a^r \rho\dot{\varepsilon}_{zz^{(n)}}\,d\rho + \frac{(r^2+a^2)}{(b^2-a^2)}\int_a^b \rho\dot{\varepsilon}_{zz^{(n)}}\,d\rho\right]$$
$$+\dot{p}_i\frac{(b^2+r^2)}{(b^2-a^2)}\frac{a^2}{r^2} - \dot{p}_0\frac{(r^2+a^2)}{(b^2-a^2)}\frac{b^2}{r^2} - E\dot{\varepsilon}_{\theta\theta^{(n)}} \quad (49)$$

where p_i and p_0 are the internal and external pressures, respectively.

Analytical differentiation with respect to the design variable (a in this case) has been carried out in order to obtain the sensitivities of the stress rates. A derivative of a typical term in the above equations has the form:

$$\frac{d}{da}\int_a^r \rho\dot{\varepsilon}_{zz^{(n)}}\,d\rho = \int_a^r \rho\mathring{\varepsilon}_{zz^{(n)}}\,d\rho + \int_a^r \frac{d\rho}{da}\dot{\varepsilon}_{zz^{(n)}}\,d\rho + \int_a^r \rho\dot{\varepsilon}_{zz^{(n)}}\overset{*}{d\rho}, \quad (50)$$

with, in this example (see Zhang and Mukherjee, 1991b)

$$\frac{d\rho}{da} = \frac{b-\rho}{b-a}, \quad \overset{*}{d\rho} = -\frac{1}{b-a}. \quad \left(\text{Note, also, } \frac{dr}{da} = \frac{b-r}{b-a}.\right)$$

The differentiation rule, used above, is the same as that used to derive the DBEM sensitivity equations such as (32).

Finally, a typical strain rate sensitivity is obtained from Hooke's law as:

$$\mathring{\varepsilon}_{\theta\theta} = \frac{1}{E}(\mathring{\sigma}_{\theta\theta} - \upsilon\mathring{\sigma}_{rr}) + \mathring{\varepsilon}_{\theta\theta^{(n)}}. \quad (51)$$

Direct solutions are obtained by integrating the rates of stresses, and stress sensitivities, in time, by using an explicit integration scheme with fixed time steps (here $\Delta t = 0.1$ s). Twenty points are used in the radial direction and the spatial integrals in eqns (48), (49) and the corresponding sensitivity equations, are obtained by Simpson's rule.

Numerical results for the standard problem and the sensitivity problem appear, respectively, in Figs 12 and 13. Figure 12 compares the DBEM and direct solutions for p_0 as a

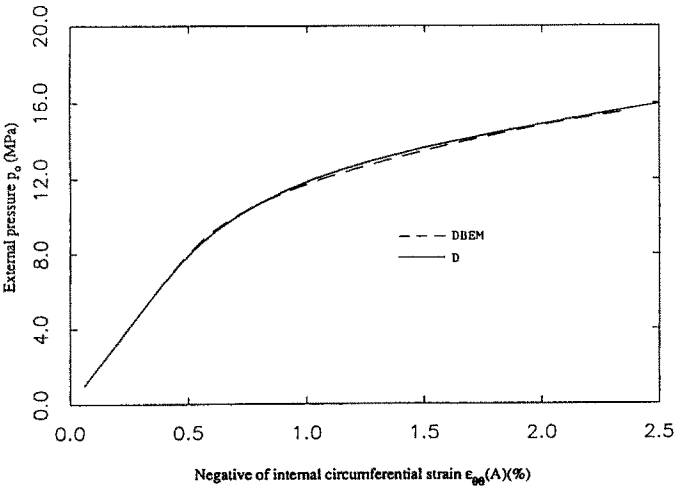

Fig. 12. External pressure as a function of $\varepsilon_{\theta\theta}(A)$ for hollow disc. $\dot{p}_0 = 5$ MPa s^{-1}, $a = 1m$, $b = 1.5m$. D: direct, DBEM: derivative BEM (from Zhang *et al.*, 1991).

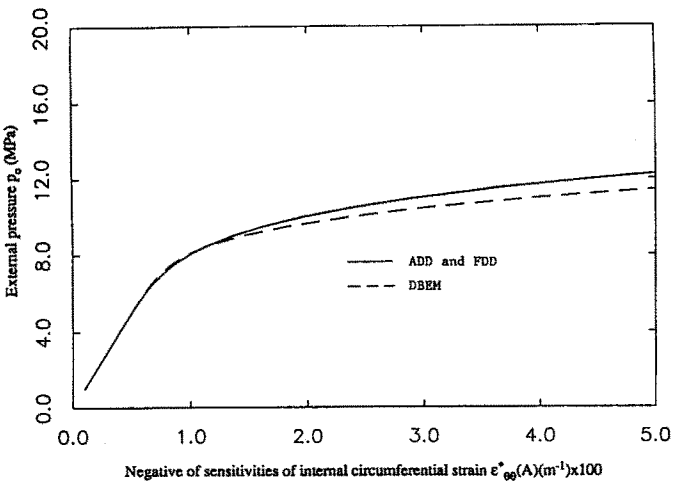

Fig. 13. External pressure as a function of $\dot{\varepsilon}^*_{\theta\theta(A)}$ for hollow disc. $\dot{p}_0 = 5$ MPa s^{-1}, $a = 1m$, $b = 1.5m$. ADD: analytical differentiation of direct solution, DBEM: derivative BEM, FDD: finite difference of direct solutions (from Zhang *et al.*, 1991).

function of $-\varepsilon_{\theta\theta}(A)$ (see Fig. 11). The agreement between the two solutions is seen to be excellent.

The external pressure p_0, as a function of $-\dot{\varepsilon}^*_{\theta\theta}(A)$, from three methods, is shown in Fig. 13. Here, as before, ADD refers to analytical differentiation of the direct solution and FDD to a finite difference of direct solutions (with $\Delta a = 0.001$). The FDD and ADD solutions coincide. The DBEM solution differs from these solutions by about 6.4% at a value of: $-\dot{\varepsilon}^*_{\theta\theta}(A) = 0.05\ \mathrm{m}^{-1}$.

4. LARGE STRAIN—LARGE ROTATION (MATERIAL AND GEOMETRIC NONLINEARITIES)

4.1. *DBEM equations for plane strain*

The two-dimensional plane strain formulation for elastic–viscoplastic problems involving small elastic strains but large inelastic strains and rotations is discussed in this section. For metallic bodies, the components of elastic strain are generally limited to about 10^{-3}, since the elastic moduli of metals are typically about three orders of magnitude larger than the yield stress. Thus, in metal forming or metal cutting operations, the nonelastic strain components, which can be of the order of unity, greatly dominate the elastic strains.

The equations are written in an updated Lagrangian frame. In this approach, the configuration of the body at time t is used as the reference frame for the deformation between time t and $t+\Delta t$. Shape design variables, however, are only defined in the original undeformed configuration and design sensitivities are obtained with respect to changes in these design variables. In other words, a superposed star on a quantity denotes its derivative with respect to a shape design variable defined in the original undeformed configuration. This aspect of the work has a total Lagrangian flavor.

4.1.1. *Boundary equations.* Using an updated Lagrangian frame, the rate form of the BEM formulation (Mukherjee and Chandra, 1987, 1991; Chandra and Mukherjee, 1984) may be written as $(i, j, k = 1, 2)$,

$$0 = \int_{\partial B} [U_{ij}(\mathbf{b}, P, Q)\tau_{i^{(L)}}(\mathbf{b}, Q) - W_{ij}(\mathbf{b}, P, Q)\delta_i(\mathbf{b}, Q)]\, \mathrm{d}s(\mathbf{b}, Q)$$

$$+ \int_B [2GU_{ij,k}(\mathbf{b}, P, q)\, \mathrm{d}_{ik^{(n)}}(\mathbf{b}, q)]\, \mathrm{d}A(\mathbf{b}, q) + \int_B U_{ij,m}(\mathbf{b}, P, q)\, g_{mi}(\mathbf{b}, q)\, \mathrm{d}A(\mathbf{b}, q), \quad (52)$$

where it is assumed that

$$d^{(n)} = d_{11}{}^{(n)} + d_{22}{}^{(n)} + d_{33}{}^{(n)} = 0 \tag{53}$$

and $\delta_i = \partial v_i / \partial s$, which, for large deformation problems, does not equal $\dot{\Delta}_i$. Here, the cross section B of the body has the boundary ∂B in the x_1–x_2 plane in a reference configuration; v_i, δ_i and $d_{ik}{}^{(n)}$ are components of velocity, its tangential derivative, and nonelastic deformation rate, respectively; and **b** denotes a vector of design variables. The quantity g_{mi} in the last domain integral may be expressed as

$$g_{mi} = \sigma_{mk}\omega_{ki} + d_{mk}\sigma_{ki} - \sigma_{mi}d_{kk}, \tag{54}$$

where the symmetric velocity gradient

$$d_{ij} = \tfrac{1}{2}(h_{ij} + h_{ji}) \tag{55}$$

and the spin

$$\omega_{ij} = \tfrac{1}{2}(h_{ij} - h_{ji}), \tag{56}$$

with $h_{ij} = v_{i,j}$. Further, $\tau_i{}^{(L)}$ denotes the components of the Lagrange traction rates which are

$$\tau_i{}^{(L)} = \tau_i{}^{(C)} - n_m g_{mi}, \tag{57}$$

with

$$\tau_i{}^{(C)} = n_m \hat{\sigma}_{mi}, \tag{58}$$

where $\tau_i{}^{(C)}$ denote the components of Cauchy traction rate with σ_{ij} the components of the Cauchy stress. A superscribed dot ($\dot{}$) denotes a material rate and a superscribed hat ($\hat{}$) denotes a corotational or Jaumann rate.

As before, a rate form of the constraint equation (10) [see, also, the equation following (24)], must be appended for some problems. It is also interesting to note that eqn (52) does not contain velocities, as in the standard BEM formulation (Mukherjee and Chandra, 1987), but, rather, velocity gradients.

4.1.2. *Stress and rotation rates on the boundary.* An extended form of eqn (25), to include the effects of large strains and rotations, has the form ($i, j, k = 1, 2$):

$$\hat{\sigma}_{ij} = A_{ijk}\tau_k{}^{(C)} + B_{ijk}\delta_k + C_{ijkl}d_{kl}{}^{(n)} + D_{ij}d_{kk}{}^{(n)}, \tag{59}$$

where A_{ijk} etc. have been defined before in eqn (25). Also,

$$h_{ij} = E_{ijk}\tau_k{}^{(C)} + F_{ijk}\delta_k + G_{ijkl}d_{kl}{}^{(n)} \tag{60}$$

where

$$E_{ijk} = \frac{c_3}{2G}n_i n_j n_k + \frac{1}{G}t_i n_j t_k$$

$$F_{ijk} = \gamma_{ij}n_k + t_i t_j t_k - c_1 n_i n_j t_k$$

and

$$G_{ijkl} = c_3 n_i n_j n_k n_l + 2t_i n_j n_k t_l$$

with $c_3 = (1-2\upsilon)/(1-\upsilon)$. The quantities c_i and γ_{ij} have been defined before in eqns (11) and (9), respectively.

The rotation rate ω_{ij} is given in terms of the velocity gradients by eqn (56).

The material rate of the Cauchy stress is obtained from the Jaumann rate from the equation

$$\dot{\sigma}_{ij} = \hat{\sigma}_{ij} - \sigma_{ik}\omega_{kj} + \omega_{ik}\sigma_{kj}. \tag{61}$$

4.1.3. *Internal equations.* Velocity gradients and stress rates are also needed at the internal points. To this end, the version of eqn (52) at an internal point is differentiated at a source point $x_i(p)$ to yield (Mukherjee and Chandra, 1991)

$$\begin{aligned} h_{jI}(\mathbf{b},p) = &\int_{\partial B} [U_{ij,I}(\mathbf{b},p,Q)\tau_{i^{(L)}}(\mathbf{b},Q) - W_{ij,I}(\mathbf{b},p,Q)\delta_i(\mathbf{b},Q)]\,\mathrm{d}s(\mathbf{b},Q) \\ &+ \frac{\partial}{\partial x_I(p)} \int_B [2GU_{ij,k}(\mathbf{b},p,q)\,\mathrm{d}_{ik^{(n)}}(\mathbf{b},q)]\,\mathrm{d}A(\mathbf{b},q) \\ &+ \frac{\partial}{\partial x_I(p)} \int_B U_{ij,m}(\mathbf{b},p,q)\,g_{mi}(\mathbf{b},q)\,\mathrm{d}A(\mathbf{b},q), \end{aligned} \tag{62}$$

where $_{,I} = \partial/\partial_I(p)$.

The boundary kernels are regular as long as p is an internal point and Q is a boundary point. This, however, is not the case for the domain integral, where a kernel which is $1/r$ singular must be differentiated again. It appears best to treat the domain integral using the technique of Huang and Du (1988). The final form of the resulting equation, which is used instead of (59), may be written as ($i, j, k, l = 1, 2$) [see eqn (26)]

$$\begin{aligned} h_{jI}(\mathbf{b},p) = &\int_{\partial B} [U_{ij,I}(\mathbf{b},p,Q)\tau_{i^{(L)}}(\mathbf{b},Q) - W_{ij,I}(\mathbf{b},p,Q)\delta_i(\mathbf{b},Q)]\,\mathrm{d}s(\mathbf{b},Q) \\ &- 2G\,\mathrm{d}_{ik^{(n)}}(\mathbf{b},p) \int_{\partial B} U_{ij,k}(\mathbf{b},p,Q)n_l(\mathbf{b},Q)\,\mathrm{d}s(\mathbf{b},Q) \\ &- g_{mi}(\mathbf{b},p) \int_{\partial B} U_{ij,m}(\mathbf{b},p,Q)n_l(\mathbf{b},Q)\,\mathrm{d}s(\mathbf{b},Q) \\ &+ \int_B 2GU_{ij,kI}(\mathbf{b},p,q)[\mathrm{d}_{ik^{(n)}}(\mathbf{b},q) - \mathrm{d}_{ik^{(n)}}(\mathbf{b},p)]\,\mathrm{d}A(\mathbf{b},q) \\ &+ \int_B U_{ij,mI}(\mathbf{b},p,q)[g_{mi}(\mathbf{b},q) - g_{mi}(\mathbf{b},p)]\,\mathrm{d}A(\mathbf{b},q). \end{aligned} \tag{63}$$

Since $[\mathrm{d}_{ik^{(n)}}(\mathbf{b},q) - \mathrm{d}_{ik^{(n)}}(\mathbf{b},p)]$ and $[g_{mi}(\mathbf{b},q) - g_{mi}(\mathbf{b},p)]$ are $O(r)$, the domain integrals are now only $1/r$ singular. Rajiyah and Mukherjee (1987) present alternate ways of treating these differentiated domain integrals.

The stress rate components at an internal point may be easily obtained from the velocity gradients and nonelastic deformation rates using the assumption that the elastic field in the problem obeys the law of hypoelasticity

$$\mathring{\sigma} = \lambda h_{kk}\delta_{ij} + \dot{G}(h_{ij}+h_{ji}) - 2G\,\mathrm{d}_{ij^{(m)}}. \tag{64}$$

Finally, the material rate of the Cauchy stress is obtained from the Jaumann rate from the eqn (61).

4.2. *Sensitivity equations for plane strain*

4.2.1. *Boundary equations.* Following Mukherjee and Chandra (1991), the first step is the differentiation of eqn (52) with respect to a design variable b. Let a superscribed asterisk(*) denote the design derivative (w.r.t. b) of a variable of interest and a superscribed circle (°) and a superscribed (°) denote design derivatives of its material rate and of its Jaumann rate, respectively, in the original undeformed configuration $\mathbf{X}^0$ (i.e. $\overset{*}{\sigma}_{ij} = \mathrm{d}\sigma_{ij}/\mathrm{d}b$, $\overset{*}{\mathring{\sigma}}_{ij} = \mathrm{d}\dot{\sigma}_{ij}/\mathrm{d}b$, $\overset{*}{\mathring{\sigma}}_{ij} = \mathrm{d}\mathring{\sigma}_{ij}/\mathrm{d}b$). Now, one obtains the equation ($i, j = 1, 2$),

$$\begin{aligned}
0 = &\int_{\partial B} [U_{ij}(\mathbf{b}, P, Q)\overset{*}{\tau}_{i^{(L)}}(\mathbf{b}, Q) - W_{ij}(\mathbf{b}, P, Q)\overset{*}{\delta}_i(\mathbf{b}, Q)]\,\mathrm{d}s(\mathbf{b}, Q) \\
&+ \int_{\partial B} [\overset{*}{U}_{ij}(\mathbf{b}, P, Q)\tau_{i^{(L)}}(\mathbf{b}, Q) - \overset{*}{W}_{ij}(\mathbf{b}, P, Q)\delta_i(\mathbf{b}, Q)]\,\mathrm{d}s(\mathbf{b}, Q) \\
&+ \int_{\partial B} [U_{ij}(\mathbf{b}, P, Q)\tau_{i^{(L)}}(\mathbf{b}, Q) - W_{ij}(\mathbf{b}, P, Q)\delta_i(\mathbf{b}, Q)]\,\overset{*}{\mathrm{d}s}(\mathbf{b}, Q) \\
&+ \int_B [2GV_{ijk}(\mathbf{b}, P, q)\,\overset{*}{\mathrm{d}}_{ik^{(m)}}(\mathbf{b}, q)]\,\mathrm{d}A(\mathbf{b}, q) \\
&+ \int_B [2G\overset{*}{V}_{ijk}(\mathbf{b}, P, q)\,\mathrm{d}_{ik^{(m)}}(\mathbf{b}, q)]\,\mathrm{d}A(b, q) \\
&+ \int_B [2GV_{ijk}(\mathbf{b}, P, q)\,\mathrm{d}_{ik^{(m)}}(\mathbf{b}, q)]\,\overset{*}{\mathrm{d}A}(\mathbf{b}, q) \\
&+ \int_B V_{ijm}(\mathbf{b}, P, q)\,\overset{*}{g}_{mi}(\mathbf{b}, q)\,\mathrm{d}A(\mathbf{b}, q) \\
&+ \int_B \overset{*}{V}_{ijm}(\mathbf{b}, P, q)\,g_{mi}(\mathbf{b}, q)\,\mathrm{d}A(\mathbf{b}, q) \\
&+ \int_B V_{ijm}(\mathbf{b}, P, q)\,g_{mi}(\mathbf{b}, q)\,\overset{*}{\mathrm{d}A}(\mathbf{b}, q).
\end{aligned} \tag{65}$$

Here, $\mathbf{b}$ is defined in the original undeformed configuration (at $t = 0$) only. The sensitivities of the kernels are:

$$\overset{*}{U}_{ij}(b, P, Q) = U_{ij,k}(b, P, Q)[\overset{*}{x}_k(Q) - \overset{*}{x}_k(P)], \tag{66}$$

$$\overset{*}{W}_{ij}(b, P, Q) = W_{ij,k}(b, P, Q)[\overset{*}{x}_k(Q) - \overset{*}{x}_k(P)], \tag{67}$$

and

$$\overset{*}{V}_{ijk}(b, P, Q) = U_{ij,kn}(b, P, Q)[\overset{*}{x}_n(Q) - \overset{*}{x}_n(P)], \tag{68}$$

where x_k are the coordinates of a material particle at a current configuration (at any time t, after updating) and $_{,k} = \partial/\partial x_k(Q)$.

The design derivative of the Lagrange traction rate may be expressed as

$$\overset{*}{\tau}_{i^{(L)}} = n_m \overset{\circ}{\overset{*}{\sigma}}_{mi} + \overset{*}{n}_m \hat{\sigma}_{mi} - \overset{*}{n}_m g_{mi} - n_m \overset{*}{g}_{mi}, \tag{69}$$

with,

$$\overset{*}{g}_{mi} = \overset{*}{\sigma}_{mk}\omega_{ki} + \overset{*}{\mathrm{d}}_{mk}\sigma_{ki} - \overset{*}{\sigma}_{mi}\mathrm{d}_{kk} + \sigma_{mk}\overset{*}{\omega}_{ki} + \mathrm{d}_{mk}\overset{*}{\sigma}_{ki} - \sigma_{mi}\overset{*}{\mathrm{d}}_{kk}. \tag{70}$$

Using Nanson's law

$$n_i H_{iM}\,\mathrm{d}s = N_{M^0}\,\mathrm{d}S^0,$$

where

$$H_{iM} = \frac{F_{iM}}{J},$$

one gets:

$$\overset{*}{n}_k = \left[-n_i \overset{*}{H}_{iM} + \overset{*}{N}{}^0_M \frac{\mathrm{d}S^0}{\mathrm{d}s} \right] H^{-1}_{Mk} - n_k \frac{\overset{*}{\mathrm{d}}s}{\mathrm{d}s} + n_k \frac{\overset{*}{\mathrm{d}}S^0}{\mathrm{d}S^0}, \tag{71}$$

where

$$\mathrm{d}S^0/\mathrm{d}s = n_i F_{i1}/JN_{1^0} = n_i F_{i2}/JN_{2^0}.$$

Also,

$$\overset{*}{\mathrm{d}}s = [\overset{*}{x}_{k,k}(Q) - n_i n_j \overset{*}{x}_{i,j}(Q)]\,\mathrm{d}s, \tag{72}$$

$$\overset{*}{\mathrm{d}}A = \overset{*}{x}_{k,k}(q)\,\mathrm{d}A, \tag{73}$$

$$\overset{*}{u}_k = \overset{*}{x}_k - \overset{*}{X}{}^0_k \tag{74}$$

and

$$\overset{*}{x}_{i,j} = \overset{*}{F}_{iM} F^{-1}_{Mj} + F_{iM} \overset{*}{X}{}^0_{M,K} F^{-1}_{Kj}, \tag{75}$$

with $F_{iJ} = \partial x_i/\partial X^0_J$ and $\overset{*}{\mathbf{F}}$ obtained by integrating:

$$\overset{*}{\dot{\mathbf{F}}} = (\overset{*}{\mathbf{d}} + \overset{*}{\omega}) \cdot \mathbf{F} + (\mathbf{d} + \omega) \cdot \overset{*}{\mathbf{F}}, \tag{76}$$

with $\overset{*}{\mathbf{F}}(0) = 0$.

At the start of the time step, half of the sensitivities $\overset{*}{\delta}_i$ and $\overset{*}{\tau}_{i^{(L)}}$ are to be determined, while all the rest of the quantities in eqn (65) are known. $\tau_{i^{(L)}}$, δ_i, $\mathrm{d}_{ij^{(n)}}$ and g_{mi} are known from a solution of the regular large strain BEM problem at this time, and the sensitivity of the nonelastic deformation rates are known from differentiating a constitutive model with state variables. Such a constitutive model is of the same form as eqns (38) and (39) with the following replacements (Mukherjee and Chandra, 1991)

$$\dot{\varepsilon}_{ij^{(n)}} \Rightarrow \mathrm{d}_{ij^{(n)}} \quad \text{and} \quad \dot{q}_{ij^{(k)}} \Rightarrow \hat{q}_{ij^{(k)}} \quad \text{in eqn (38)}$$

and

$$\mathring{\varepsilon}_{ij^{(n)}} \Rightarrow \overset{*}{\mathrm{d}}_{ij^{(n)}} \quad \text{and} \quad \mathring{q}_{ij^{(k)}} \Rightarrow \mathring{\overset{*}{q}}_{ij^{(k)}} \quad \text{in eqn (39).}$$

For large strain problems, $\tau_{i^{(l)}}$ and g_{mi} contain velocity gradients, whose design sensitivities are not known *a priori*. Thus, like usual large strain problems (Mukherjee and Chandra, 1987), iterations will be needed in order to solve eqn (65). The quantities $\overset{*}{x}_{i,j}$ must be obtained from eqn (75) and used to find $\mathrm{d}\overset{*}{s}/\mathrm{d}s$ and $\mathrm{d}\overset{*}{A}/\mathrm{d}A$. For this, the time histories of $\mathbf{F}$ and $\overset{*}{\mathbf{F}}$ must be tracked during the deformation process. Finally, $\overset{*}{\mathbf{x}}$ can be obtained by integrating $\overset{*}{x}_{i,j}$; and $\overset{*}{\mathbf{u}}$ from eqn (74).

4.2.2. *Stress and rotation rate sensitivities on the boundary.* The sensitivity equations for rates on the boundary are

$$\mathring{\overset{*}{\sigma}}_{ij} = A_{ijk}\overset{*}{\tau}_{k^{(C)}} + B_{ijk}\overset{*}{\delta}_k + C_{ijkl}\overset{*}{\mathrm{d}}_{kl^{(n)}} + D_{ij}\overset{*}{\mathrm{d}}_{kk^{(n)}} + \overset{*}{A}_{ijk}\tau_{k^{(C)}} + \overset{*}{B}_{ijk}\delta_k + \overset{*}{C}_{ijkl}\mathrm{d}_{kl^{(n)}} + \overset{*}{D}_{ij}\mathrm{d}_{kk^{(n)}}, \tag{77}$$

$$\overset{*}{h}_{ij} = E_{ijk}\overset{*}{\tau}_{k^{(C)}} + F_{ijk}\overset{*}{\delta}_k + G_{ijkl}\overset{*}{\mathrm{d}}_{kl^{(n)}} + \overset{*}{E}_{ijk}\tau_{k^{(C)}} + \overset{*}{F}_{ijk}\delta_k + \overset{*}{G}_{ijkl}\mathrm{d}_{kl^{(n)}}, \tag{78}$$

$$\mathring{\sigma}_{ij} = \mathring{\overset{*}{\sigma}}_{ij} - \overset{*}{\sigma}_{ik}\omega_{kj} - \sigma_{ik}\overset{*}{\omega}_{kj} + \overset{*}{\omega}_{ik}\sigma_{kj} + \omega_{ik}\overset{*}{\sigma}_{kj}. \tag{79}$$

4.2.3. *Internal equations.* A sensitivity equation from (63), for the sensitivities of velocity gradients (and hence stress rates) at an internal point, may be written as (all indices 1, 2):

$$\begin{aligned}
\overset{*}{h}_{jI}(\mathbf{b}, p) = & \int_{\partial B} [V_{ijI}(\mathbf{b}, p, Q)\overset{*}{\tau}_{i^{(L)}}(\mathbf{b}, Q) - Y_{ijI}(\mathbf{b}, p, Q)\overset{*}{\delta}_i(\mathbf{b}, Q)]\,\mathrm{d}s(\mathbf{b}, Q) \\
& + \int_{\partial B} [\overset{*}{V}_{ijI}(\mathbf{b}, p, Q)\tau_{i^{(L)}}(\mathbf{b}, Q) - \overset{*}{Y}_{ijI}(\mathbf{b}, p, Q)\delta_i(\mathbf{b}, Q)]\,\mathrm{d}s(\mathbf{b}, Q) \\
& + \int_{\partial B} [V_{ijI}(\mathbf{b}, p, Q)\tau_{i^{(L)}}(\mathbf{b}, Q) - Y_{ijI}(\mathbf{b}, p, Q)\delta_i(\mathbf{b}, Q)]\,\overset{*}{\mathrm{d}}s(\mathbf{b}, Q) \\
& - 2G\overset{*}{\mathrm{d}}_{ik^{(n)}}(\mathbf{b}, p)\int_{\partial B} V_{ijk}(\mathbf{b}, p, Q)n_l(\mathbf{b}, Q)n_l(\mathbf{b}, Q)\,\mathrm{d}s(\mathbf{b}, Q) \\
& - 2G\,\mathrm{d}_{ik^{(n)}}(\mathbf{b}, p)\int_{\partial B} \overset{*}{V}_{ijk}(\mathbf{b}, p, Q)\,\mathrm{d}s(\mathbf{b}, Q) \\
& - 2G\,\mathrm{d}_{ik^{(n)}}(\mathbf{b}, p)\int_{\partial B} V_{ijk}(\mathbf{b}, p, Q)\overset{*}{n}_l(\mathbf{b}, Q)\,\mathrm{d}s(\mathbf{b}, Q) \\
& - 2G\,\mathrm{d}_{ik^{(n)}}(\mathbf{b}, p)\int_{\partial B} V_{ijk}(\mathbf{b}, p, Q)n_l(\mathbf{b}, Q)\,\overset{*}{\mathrm{d}}s(\mathbf{b}, Q) \\
& - \overset{*}{g}_{mi}(\mathbf{b}, p)\int_{\partial B} U_{ij,m}(\mathbf{b}, p, Q)n_l(\mathbf{b}, Q)\,\mathrm{d}s(\mathbf{b}, Q) \\
& - g_{mi}(\mathbf{b}, p)\int_{\partial B} \overset{*}{V}_{ijm}(\mathbf{b}, p, Q)n_l(\mathbf{b}, Q)\,\mathrm{d}s(\mathbf{b}, Q) \\
& - g_{mi}(\mathbf{b}, p)\int_{\partial B} V_{ijm}(\mathbf{b}, p, Q)\overset{*}{n}_l(\mathbf{b}, Q)\,\mathrm{d}s(\mathbf{b}, Q) \\
& - g_{mi}(\mathbf{b}, p)\int_{\partial B} V_{ijm}(\mathbf{b}, p, Q)n_l(\mathbf{b}, Q)\,\overset{*}{\mathrm{d}}s(\mathbf{b}, Q)
\end{aligned}$$

$$+\int_B 2G\overset{*}{P}_{ijkl}(\mathbf{b},p,q)\,[\mathrm{d}_{ik^{(n)}}(\mathbf{b},q)-\mathrm{d}_{ik^{(n)}}(\mathbf{b},p)]\,\mathrm{d}A(\mathbf{b},q)$$

$$+\int_B 2GP_{ijkl}(\mathbf{b},p,q)\,[\overset{*}{\mathrm{d}}_{ik^{(n)}}(\mathbf{b},q)-\overset{*}{\mathrm{d}}_{ik^{(n)}}(\mathbf{b},p)]\,\mathrm{d}A(\mathbf{b},q)$$

$$+\int_B 2GP_{ijkl}(\mathbf{b},p,q)\,[\mathrm{d}_{ik^{(n)}}(\mathbf{b},q)-\mathrm{d}_{ik^{(n)}}(\mathbf{b},p)]\,\overset{*}{\mathrm{d}A}(\mathbf{b},q)$$

$$+\int_B \overset{*}{P}_{ijml}(\mathbf{b},p,q)[g_{mi}(\mathbf{b},q)-g_{mi}(\mathbf{b},p)]\,\mathrm{d}A(\mathbf{b},q)$$

$$+\int_B P_{ijml}(\mathbf{b},p,q)[\overset{*}{g}_{mi}(\mathbf{b},q)-\overset{*}{g}_{mi}(\mathbf{b},p)]\,\mathrm{d}A(\mathbf{b},q)$$

$$+\int_B P_{ijml}(\mathbf{b},p,q)[g_{mi}(\mathbf{b},q)-g_{mi}(\mathbf{b},p)]\,\overset{*}{\mathrm{d}A}(\mathbf{b},q). \tag{80}$$

Although this eqn (80) is long, it may be easily evaluated. The boundary kernels are regular and the domain integrands are $1/r$ singular. These domain integrals can be accurately evaluated by standard means (e.g. Mukherjee, 1982). The entire right hand side of eqn (80) is known at this stage except for the integrals involving $\overset{*}{g}_{mi}$, which depend on $\overset{*}{h}_{ij}$. Accordingly, iterations are needed over eqns (65) and (80). These iterations are similar to those needed over velocity gradients for BEM analyses of large strain problems.

Finally, the stress rate sensitivities at an internal point are evaluated from the equation below which is obtained by differentiating the hypoelastic law (64) with respect to b

$$\overset{\circ}{\bar{\sigma}} = \lambda\overset{*}{h}_{kk}\delta ij+G(\overset{*}{h}_{ij}+\overset{*}{h}_{ji})-2G\,\overset{*}{\mathrm{d}}_{ij^{(n)}}, \tag{81}$$

together with eqn (79) for $\mathring{\sigma}_{ij}$.

4.3. *Modelling of corners for plane strain*

In certain special situations the stress tensor, and therefore its material rate, remains continuous at a corner throughout the deformation history. An example is a right angled corner in which the corner angle remains a right angle throughout a deformation process. Another example is a corner which arises from using symmetry in a problem where the point was originally regular. In such cases, one can write corner equations in a manner analogous to the cases which have been considered before in this chapter, i.e.

$$\dot{\sigma}_{ij}^{-} = \dot{\sigma}_{ij}^{+}, \tag{82}$$

where $\dot{\sigma}_{ij}$, on either side of the corner, is obtained from eqns (59), (60) and (61), together with (56), as functions of components $\tau^{(c)}$, δ, $\mathbf{d}^{(n)}$ and σ as well as υ, G, $\mathbf{n}$ and $\mathbf{t}$. In this case the corner sensitivity equation is of the form

$$\mathring{\sigma}_{ij}^{-} = \mathring{\sigma}_{i+j}^{+}. \tag{83}$$

A possible option for the general case is to invoke continuity of the velocity $\mathbf{v}$ at a corner. This leads to integral constraints as shown below. Suppose that AC and CB are

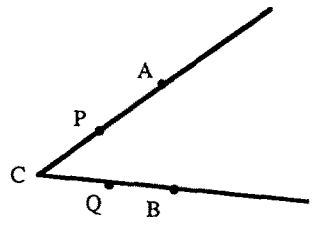

Fig. 14.

two smooth segments that meet at a corner C (Fig. 14). Then, continuity of $\mathbf{v}$ at C demands that

$$v_i(P)+\int_P^C \delta_i^- \, ds = v_i(Q)-\int_C^Q \delta_i^+ \, ds \tag{84}$$

where P within AC and Q within CB are points at which the velocities are known. Of course, if velocities are not known at any point within smooth segments contiguous to a corner, then velocity information from points further away must be used and eqn (84) must be suitably modified. Knowledge of $\mathbf{v}$ at any one point on ∂B is sufficient for this idea to work.

Equation (84) gives two equations at each corner, and this extra information is sufficient to solve the problem. The sensitivity equation corresponding to (84) has the form:

$$\overset{*}{v}_i(P)+\int_P^C \overset{*}{\delta}_i^- \, ds+\int_P^C \delta_i^- \, \overset{*}{ds} = \overset{*}{v}_i(Q)-\int_C^Q \overset{*}{\delta}_i^+ \, ds-\int_C^Q \delta_i^+ \, \overset{*}{ds}. \tag{85}$$

A word of caution here. Sometimes, as discussed in detail in Zhang and Mukherjee (1991a) Δ_n and associated rotations can become singular at a corner. In such cases, care must be exercised in using eqns (84) and (85) in the general case. Suitable shape functions for Δ_n, to reflect this singular behavior, must be employed.

4.4. *Solution algorithm*

The solution algorithm for large strain elastic–viscoplastic problems, which involves solutions of appropriate equations at the beginning of each time step and then marching forward in time, is discussed in detail in several previous papers (Chandra and Mukherkee, 1984; Mukherjee and Chandra, 1987, 1991). Iterations are needed, since the velocity gradients appearing in eqn (52) (in a domain integral and in the boundary integral through $\tau_{j(i)}$), are not known *a priori*. One important advantage of this DBEM formulation over the usual BEM formulation (Mukherjee and Chandra, 1987) is that velocity components do not appear, by themselves, in these equations and that the boundary velocity gradients can be directly evaluated from eqn (60).

Sensitivity calculations must also be carried out using a procedure analogous to that of the usual large strain problem. Also, this must be done in parallel with the usual problem. Iterations over sensitivities of velocity gradients are now needed. The algorithm for the sensitivity problem is described below (Mukherjee and Chandra, 1991).

The solution for sensitivities at the initial time is obtained by solving the appropriate elasticity equations. Figure 15 illustrates the procedure for moving to $t+\Delta t$ when the solution up to time t is known. The BEM equation (65) is first solved in order to obtain the unknown values of $\overset{*}{\delta}_i$ and $\overset{*}{\tau}_{j(i)}$ on ∂B using an estimated value for sensitivities of velocity gradients. Now, the boundary algebraic equations (77–79) are used to determine $\overset{*}{\sigma}_{ij}$ and $\overset{*}{h}_{ij}$ on ∂B. Next, the internal BEM equation (80) is used to obtain $\overset{*}{h}_{ij}$ at selected internal points, and the law of hypoelasticity (81) is used to obtain the stress rate sensitivities at these internal points. The new values of $\overset{*}{h}_{ij}$ on ∂B and in B are now incorporated into eqn (65), and the system of eqns (65, 77–79 and 80–81, as well as the sensitivity equations from

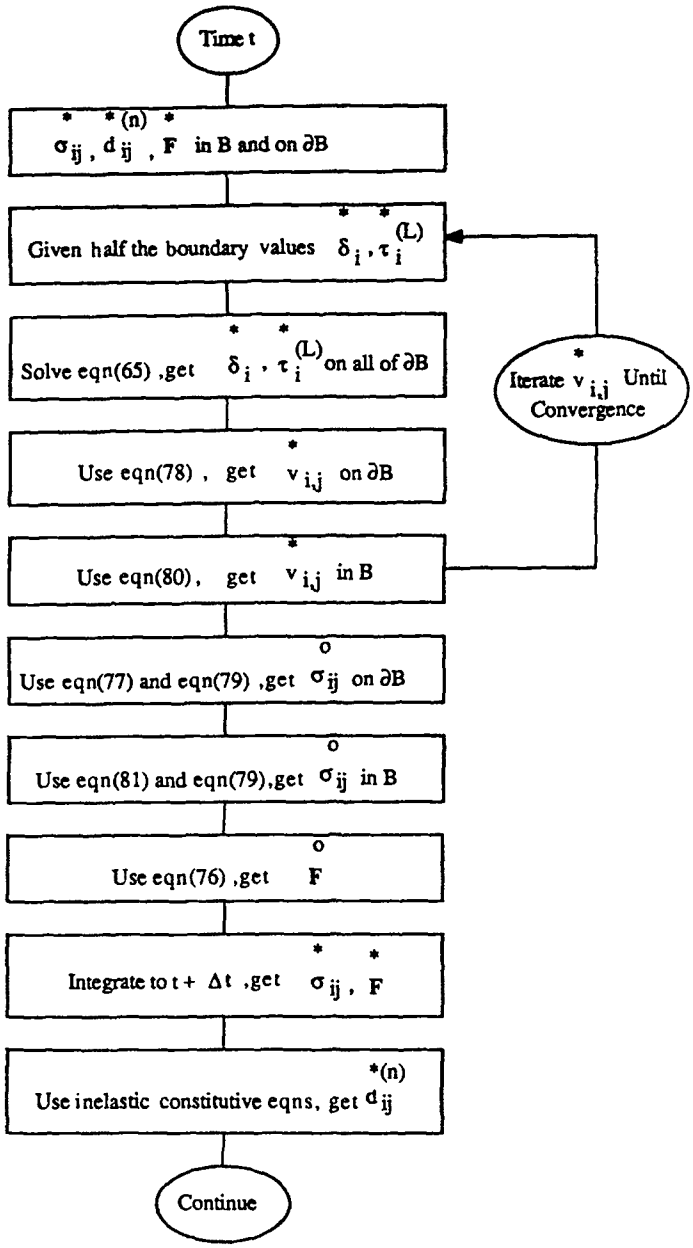

Fig. 15. Algorithm for advancing the sensitivity solution from time t to $t+\Delta t$.

a material constitutive model) is solved with the new right hand side and iterated until convergence. It is important to note here that the kernels and the coefficient matrices need not be altered during iterations. The rates including $\overset{o}{F}$ are integrated to obtain the sensitivities of the relevant quantities at time $t+\Delta t$. The constitutive equations are not used to calculate $\overset{*}{d}_{ij^{(n)}}$ at $t+\Delta t$ from the values and sensitivities of the stresses and state variables at this time. For classical elastic–plastic material models, $\overset{*}{d}_{ij^{(n)}}$ depends on $\overset{o}{\sigma}_{ij}$, as well as on the stress components and their sensitivities. This requires iterations over $\overset{*}{d}_{ij^{(n)}}$ within each time step. The sensitivity problem, however, still has approximately the same level of complexity as the original elastic–plastic problem. For large strain problems, iterations over $\overset{*}{d}_{ij^{(n)}}$ may be carried out within the iteration scheme for $\overset{*}{h}_{ij}$.

Thus, large strain sensitivity problems of elastoplasticity and elastoviscoplasticity are expected to require approximately twice the computational effort needed for the regular

BEM analysis including both geometric and material nonlinearities when sensitivity with respect to one design variable is needed. In a typical design environment, however, sensitivities with respect to a large number of design variables are desired. It is interesting to note here that the determination of sensitivities with respect to additional design variables does not require solutions of new matrix systems. The coefficient matrices remain the same for all cases, only the right hand side changes. Hence, for the slight increase in additional costs due to additional evaluations of the right hand side, it is possible to simultaneously track the sensitivities with respect to several design variables.

5. CONCLUDING REMARKS

Numerical results for DSCs for elasticity problems and first results for DSCs for materially nonlinear problems (elastoviscoplastic), obtained by direct differentiation of the relevant boundary integral equations, have been presented in this paper. Although these first numerical examples for nonlinear problems have simple geometry, it is very encouraging to see that the sensitivities are obtained accurately over the entire history of the elastoviscoplastic deformation process.

It is important to remember here that strain rates in elastoplastic or elastoviscoplastic problems are typically strongly dependent on stresses. Thus, there is usually a stronger requirement on the accuracy of numerically calculated stresses in these nonlinear problems, compared to that for linear elastic problems. Further, sensitivities are derivatives of history dependent quantities. Thus, overall, the DBEM must be implemented numerically with great care in order to fully exploit the intrinsic accuracy of the boundary element method. In particular, very accurate numerical evaluation of singular integrals is crucial for successful solution of these problems. Thus, for example, a half percent inaccuracy in calculating log-singular integrals was found to be intolerable even for the simple example of one-dimensional straining of a square made of an elastoviscoplastic material. Also, Gaussian integration rules for $1/r$ singular integration in two-dimensional domains (that have been reported in the literature) were found to be of unacceptable accuracy for these problems and mappings in order to make these integrals regularly used.

These first results for DSCs for materially nonlinear problems are extremely encouraging. As mentioned in the introduction, DSCs are useful for diverse applications such as evaluating the robustness of a given design, solving of inverse problems etc. The primary goal of this ongoing research program, however, is the use of these DSCs in the optimal design of nonlinear processes in solid mechanics. One aspect of this work is to use the DSCs obtained here to carry out optimal shape design in the presence of material nonlinearities (small strain elastoplastic or elastoviscoplastic problems). A possible application is shape design of, say, a pressure vessel, to optimize the residual stress distribution due to initial overpressurization.

The work on DSCs for fully nonlinear (material as well as geometric) problems is expected to have exciting applications in the optimal design of manufacturing processes. Examples are the design of optimal die shapes for extrusion or optimal preform shapes for forging. Such problems are extremely challenging. They are, also, of great technological importance and the potential rewards from solving these problems are indeed very substantial.

Acknowledgements—The research reported in this paper has been supported by NSF grants numbers MSM-8609391 to Cornell University and MSS-8922185 to Cornell University and the University of Arizona. The computing has been supported by the Cornell National Supercomputer Facility.

REFERENCES

Aithal, R., Saigal, S. and Mukherjee, S. (1990). Three-dimensional boundary element implicit differentiation formulation for design sensitivity analysis. *Math. Comput. Model.* **15,** 1–10 (In press).

Anand, L. (1982). Constitutive equations for the rate-dependent deformation of metals at elevated temperatures. *ASME J. Engng Mater. Technol.* **104,** 12–17.

Ang, A. H.-S. and Tang, W. H. (1975). *Probability Concepts in Engineering Planning and Design.* Wiley, New York.

Barone, M. R. and Yang, R.-J. (1988). Boundary integral equations for recovery of design sensitivities in shape optimization. *AIAA J.* **26,** 589–594.
Barone, M. R. and Yang, R.-J. (1989). A boundary element approach for recovery of shape sensitivities in three-dimensional elastic solids. *Comput. Meth. Appl. Mech. Engng* **74,** 69–82.
Cardoso, J. B. and Arora, J. S. (1988). Variational methods for design sensitivity analysis in nonlinear structural mechanics. *AIAA J.* **26,** 595–602.
Chandra, A. and Mukherjee, S. (1984). Boundary element formulations for large strain deformation problems of viscoplasticity. *Int. J. Solid Structures* **20,** 41–53.
Cristescu, M. and Loubignac, G. (1978). Gaussian quadrature formulations for functions with singularities in $1/r$ over triangles and quadrangles. In *Recent Advances in Boundary Element Methods* (Edited by C. A. Brebbia), pp. 375–390. Pentech Press, London.
Cruse, T. A. and Vanburen, W. (1971). Three-dimensional elastic stress analysis of a fracture specimen with an edge crack. *Int. J. Fracture Mech.* **7,** 1–15.
Ghosh, N. and Mukherjee, S. (1987). A new boundary element method formulation for three-dimensional problems in linear elasticity. *Acta Mechanics* **67,** 107–119.
Ghosh, N., Rajiyah, H., Ghosh, S. and Mukherjee, S. (1986). A new boundary element method formulation for linear elasticity. *ASME J. Appl. Mech.* **53,** 69–76.
Golub, G. H. and Van Loan, C. F. (1989). *Matrix Computations.* The Johns Hopkins University Press, Baltimore and London.
Haug, E. J., Choi, K. K. and Komkov, V. (1986). *Design Sensitivity Analysis of Structural Systems.* Academic Press, New York.
Kane, J. H. and Saigal, S. (1988). Design sensitivity analysis of solids using BEM. *ASCE J. Engng Mech.* **114,** 1703–1722.
Mukherjee, S. (1977). Corrected boundary-integral equations in planar thermoelastoplasticity. *Int. J. Solids Structures* **13,** 331–335.
Mukherjee, S. (1982). *Boundary Element Methods in Creep and Fracture.* Elsevier Applied Science, London.
Mukherjee, S. and Chandra, A. (1987). Nonlinear solid mechanics. In *Boundary Element Methods in Mechanics,* Vol. 3 in Computational Methods in Mechanics (Edited by D. E. Beskos), pp. 285–331. Elsevier Sience Publishers, Amsterdam.
Mukherjee, S. and Chandra, A. (1989). A boundary element formulation for design sensitivities in materially nonlinear problems. *Acta Mechanica* **78,** 243–253.
Mukherjee, S. and Chandra, A. (1991). A boundary element formulation for design sensitivities in problems involving both geometric and material nonlinearities. *Math. Comput. Model.* **15,** 245–255.
Okada, H., Rajiyah, H. and Atluri, S. N. (1988). A novel displacement gradient boundary element method for elastic stress analysis with high accuracy. *ASME J. Appl. Mech.* **55,** 786–794.
Pina, H. L. G., Fernandes, J. L. M. and Brebbia, C. A. (1981). Some numerical integration formulae over triangle and squares with a $1/r$ singularity. *Appl. Math. Model.* **5,** 209–211.
Rice, J. R. and Mukherjee, S. (1990). Design sensitivity coefficients for axisymmetric elasticity problems by boundary element methods. *Engng Anal. Boundary Elements* **7,** 13–20.
Rizzo, F. J. (1967). An integral equation approach to boundary value problems of classical elastostatics. *Q. Appl. Math.* **25,** 83–95.
Saigal, S., Borggaard, J. T. and Kane, J. H. (1989). Boundary element implicit differentiation equations for design sensitivities of axisymmetric structures. *Int. J. Solid Structures* **25,** 527–538.
Sladek, J. and Sladek, V. (1986). Computation of stresses by BEM in 2D elastostatics. *Acta Structures* **31,** 523–531.
Tortorelli, D. A. (1988). Design sensitivity analysis for nonlinear dynamic thermoelastic systems, Ph.D. Thesis, University of Illinois at Urbana Champaign.
Tortorelli, D. A. (1990). Sensitivity analysis for nonlinear constrained elastostatic systems. *Symp. on Design Sensitivity Analysis and Shape Optimization Using Numerical Methods* (Edited by S. Saigal and S. Mukherjee), pp. 115–126. ASME, New York.
Tsay, J. J. and Arora, J. S. (1990). Nonlinear structural design sensitivity analysis for path dependent problems, part 1: general theory. *Comput. Meth. Appl. Mech. Engng* **81,** 183–208.
Tsay, J. J., Cardoso, J. E. B. and Arora, J. S. (1990). Nonlinear structural design sensitivity analysis for path dependent problems, part 2: analytical examples. *Comput. Meth. Appl. Mech. Engng* **81,** 209–228.
Vanderplaats, G. N. (1983). *Numerical Optimization Techniques for Engineering Design.* McGraw-Hill, New York.
Williams, M. L. (1952). Stress singularities resulting from various boundary conditions in angular corners of plates in extension. *ASME J. Appl. Mech.* **19,** 526–528.
Wu, C. C. and Arora, J. S. (1987) Design sensitivity analysis and optimization of nonlinear structure response using incremental procedure. *AIAA J.* **25,** 1118–1125.
Zabaras, N., Mukherjee, S. and Richmond, O. (1988). An analysis of inverse heat transfer problems with phase changes using an integral method. *ASME J. Heat Transfer* **110,** 554–561.
Zhang, Q. and Mukherjee, S. (1991a). Design sensitivity coefficients for linear elastic bodies with zones and corners by the derivative boundary element method. *Int. J. Solids Structures* **27,** 983–998.
Zhang, Q. and Mukherjee, S. (1991b). Second-order design sensitivity analysis for linear elastic problems by the derivative boundary element method. *Computer Methods in Applied Mechanics and Engineering.* (In press.)
Zhang, Q., Mukherjee, S. and Chandra, A. (1991) Design sensitivity coefficients for elasto-viscoplastic problems by boundary element methods. *Int. J. Numer. Meth. Engng.* (In press.)